An Electrolyte CPA Equation of State for Mixed Solvent Electrolytes

Bjørn Maribo-Mogensen, Kaj Thomsen, and Georgios M. Kontogeorgis
Center for Energy Resources Engineering, Department of Chemical and Biochemical Engineering, Technical University of Denmark (DTU), Lyngby, Denmark

DOI 10.1002/aic.14829
Published online August 7, 2015 in Wiley Online Library (wileyonlinelibrary.com)

Despite great efforts over the past decades, thermodynamic modeling of electrolytes in mixed solvents is still a challenge today. The existing modeling frameworks based on activity coefficient models are data-driven and require expert knowledge to be parameterized. It has been suggested that the predictive capabilities could be improved through the development of an electrolyte equation of state. In this work, the Cubic Plus Association (CPA) Equation of State is extended to handle mixtures containing electrolytes by including the electrostatic contributions from the Debye–Hückel and Born terms using a self-consistent model for the static permittivity. A simple scheme for parameterization of salts with a limited number of parameters is proposed and model parameters for a range of salts are determined from experimental data of activity and osmotic coefficients as well as freezing point depression. Finally, the model is applied to predict VLE, LLE, and SLE in aqueous salt mixtures as well as in mixed solvents. © 2015 American Institute of Chemical Engineers *AIChE J*, 61: 2933–2950, 2015
Keywords: aqueous solutions, thermodynamics/classical, electrochemistry

Introduction

Complex mixtures containing hydrogen-bonding, polar, nonpolar components, and electrolytes are ubiquitous in biology and are also important to many industrial processes, such as acid gas cleaning, waste-water treatment, energy storage in batteries, desalination, fractional crystallization, extractive distillation, as well as bio-separations. Chemical engineers require knowledge of the physical properties of chemical compounds in mixtures and of the partition coefficients in multiphase systems over wide ranges of temperatures and pressures to accurately design and optimize production of chemicals and energy. This knowledge requires obtaining high-quality experimental data at different conditions, combined with accurate, predictive thermodynamic models that can represent the phase behavior and thermal properties of the fluid.[1]

Throughout the last century, scientists and engineers have developed physical models to account for the thermodynamics of complex mixtures. Successful modeling concepts, such as activity coefficient models (e.g. the NRTL or UNIQUAC models) or the equations of state (EoS) based on the van der Waals model, or the Statistical Associating Fluid Theory enable an accurate prediction of phase distribution of chemicals over wide ranges of temperature and pressure for complex chemicals.[2] Process simulators generally provide engineers with many choices of thermodynamic models to describe the chemicals of interest.[3] When electrolytes are present, the choices are drastically limited to activity coefficient models such as the electrolyte NRTL, OLI mixed solvent electrolyte, and Pitzer equations.[4–6]

One of the major conclusions from a large survey performed by the Working Party for Thermodynamic and Transport Properties of the European Federation of Chemical Engineers (EFCE) was that the current models are inadequate, as the predictive capabilities are limited and that electrolyte models generally require more parameters and perform much worse than the nonelectrolyte counterparts.[1] New models must be able to handle all types of phase behavior (VLE/LLE/SLE) and thermal properties of electrolytes in mixed solvents with hydrocarbons over extensive temperature and pressure ranges.[1] The difficulties and challenges associated with electrolyte thermodynamics are extensively discussed in the excellent monograph by Prausnitz et al.[7]

Throughout the last three decades, many different approaches to the development of an electrolyte EoS have been suggested by scientists in the field in an effort to improve the modeling capabilities for mixtures containing electrolytes.[1] Still, EoS-based modeling of mixtures containing electrolytes remains a challenging task, and as most of the approaches presented in literature are focusing on aqueous solutions they cannot easily be extended to handle mixed solvents.[2] Furthermore, the approaches suggested in current literature have rarely been applied to all types of thermodynamic equilibrium calculations relevant to electrolyte solutions.

*Current address of Bjørn Maribo-Mogensen: Linde AG – Engineering Division,, IT for Process Design and Control, ITP, Dr.-Carl-von-Linde-Str. 6-14, D-82049, Pullach, Germany

Correspondence concerning this article should be addressed to G. M. Kontogeorgis at gk@kt.dtu.dk.

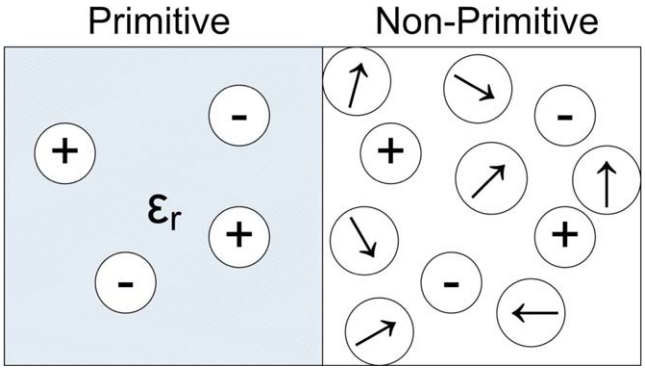

Figure 1. Fluid representation in the primitive and the nonprimitive models for the electrostatic interactions.

[Color figure can be viewed in the online issue, which is available at wileyonlinelibrary.com.]

The general approach used by researchers to develop electrolyte EoS is to extend the model for the Helmholtz free energy of the fluid to account for the electrostatic interactions; however, researchers disagree on how this should be done. The electrostatic ion-ion interactions have most often been described from the primitive approach using the Debye–Hückel[8] or the mean spherical approximation (MSA)[9] models, where ions are immersed in a continuum solvent with static permittivity ε_r, but recently, Herzog et al.[10] presented results with an EoS based on the nonprimitive mean spherical approximation model, which explicitly accounts for all ion-ion, ion-dipole, and dipole-dipole interactions. The difference between these approaches is illustrated in Figure 1.

The main advantage of the nonprimitive modeling approach is that it does not require a model for the static permittivity. Still, as the nonprimitive approach requires the inclusion of dipole-dipole interactions, it is incompatible with most modern equations of state, such as the PC-SAFT and CPA that do not explicitly account for the dipole-dipole interactions. Even accounting for the polar interactions in today's models is not entirely satisfactory.[2] The PC-SAFT or the CPA EoS may still be extended to handle electrolytes using the primitive models, and as evidenced by the authors' analysis of the Debye–Hückel and MSA models, either model can be used.[11]

The concept of implicitly accounting for the effect of the solvent dates back to the pioneering work by van't Hoff, who received the Nobel prize for his work on establishing the thermodynamics of solutes through the concept of the osmotic pressure.[12] The first formal statistical mechanical treatment was developed by McMillan and Mayer,[13] who transformed the Grand canonical partition function into an effective form involving only solute species and where the solvent effect enters through effective solute-solute interaction potentials. Adelman[14,15] derived a solute-based Ornstein–Zernike relation and showed that when this relation was applied to electrostatic interactions, it provides a relationship between the primitive and nonprimitive models. In this equation, the effective ion-ion interaction potentials are shielded by the static permittivity of the fluid, as calculated from the direct and indirect dipole-dipole correlation functions of all compounds in the mixture as shown in Eq. 1 for the Fourier transformed direct ion-ion correlation function between ion i and j with charge q_i

$$(2\pi)^{3/2} c_{ij}^{\text{eff}}(k) = \frac{q_i q_j}{k_B T \varepsilon_r \varepsilon_0 k^2} \tag{1}$$

In the limit of infinite dilution, the static permittivity can be calculated from the model by Wertheim[16] using the direct correlation functions of the dipole-dipole interactions. This insight was used by Liu et al.[17,18] who developed an electrolyte EoS, where the static permittivity was calculated from the Wertheim model for the static permittivity and the MSA model for ion-ion interactions.

In addition to the ion-ion interactions, another important characteristic of electrolyte mixtures is that ions tend to go toward the phase with the highest static permittivity. A consequence of this is that ions display a large negative value of the Gibbs energy of hydration, and this effect may be modeled using the Born term,[19] or from the ion-dipole interactions in the nonprimitive MSA.[10] While some researchers have included a Born model in the electrolyte EoS,[20] it has been often omitted from published electrolyte EoS. A common argument for omitting the Born term is that it will not provide a contribution to the activity coefficients—however, this is only the case when the model for the static

Table 1. Ion-Specific Parameters and Hydration Enthalpies at 25°C Used in This Study Calculated from Wagman et al.[44] and Mejias and Lago[43]: Note that b_i was Calculated from d_i, and that the Born Radius was then Adjusted to Match the Enthalpy of Hydration at 25°C for all Salts

	$\Delta_f H^{ig}$ (kJ/mol)	$\Delta_{\text{hyd}} H$ (kJ/mol)	d_i (Å)	b_i (cm^3/mol)	R_{Born} (Å)
H^+	1536.202	−1150.1	1.10	1.679	0.643
Li^+	685.783	−578.167	2.08	11.35	1.319
Na^+	609.358	−463.375	2.36	16.49	1.665
K^+	514.26	−380.534	2.78	27.62	2.065
Rb^+	490.101	−355.162	2.89	30.44	2.256
Cs^+	457.964	−330.138	3.14	39.01	2.432
Mg^{++}	2348.504	−2043.15	2.09	11.51	1.443
Ca^{++}	1925.9	−1696.52	2.42	17.91	1.759
Sr^{++}	1790.54	−1564.13	2.64	23.02	1.902
Ba^{++}	1660.38	−1425.82	3.00	34.05	2.152
F^-	−255.39	−463.344	2.63	22.94	1.411
Cl^-	−228.61	−324.645	3.19	40.83	1.828
Br^-	−219.07	−288.579	3.37	48.40	2.059
I^-	−197	−244.292	3.65	61.18	2.460
OH^-	−143.5	−472.598	2.66	23.73	1.397
NO_3^-	−306.16	−287.303	3.16	39.80	2.050
SO_4^-	−634.561	−1046.92	3.82	70.03	2.415

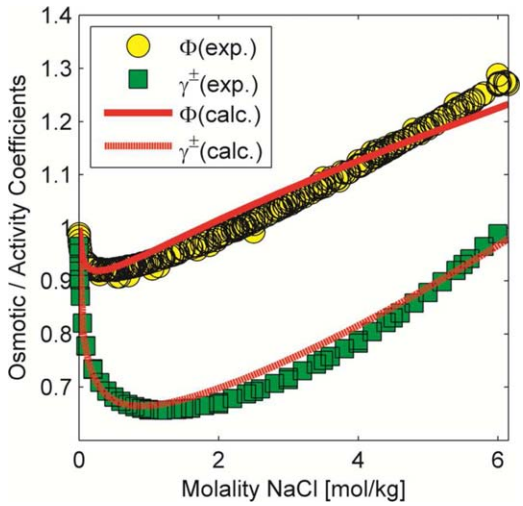

Figure 2. Correlated osmotic coefficients and activity coefficients for NaCl in water at 25°C using the parameters from Tables 1–3.

[Color figure can be viewed in the online issue, which is available at wileyonlinelibrary.com.]

permittivity is assumed to be independent of the mixture composition, as illustrated by, for example, Inchekel et al.[21]

In a recent publication [11], the authors showed that in the case of primitive models such as the Debye–Hückel and Born terms, the choice of a physically correct model for the static permittivity is of high importance,[11] and that the choice of empirical correlations (as used in most published electrolyte EoS) may lead to unphysical behavior of the EoS. In two subsequent articles,[22,23] a new theoretical model was developed to extend the framework by Onsager,[24] Kirkwood,[25] and Frölich[26] for modeling of the static permittivity to hydrogen-bonding compounds and salts. The new model uses a simplified geometrical configuration of the dipolar molecules in a hydrogen-bonding network to describe the short-range dipolar correlations, and relies on the Wertheim association theory as used in the SAFT-based equations of state to determine the probability of association between different molecules. It was shown that the new model accurately predicts the static permittivity of mixtures containing hydrogen-bonding, polar, and nonpolar compounds as well as ions over wide ranges of temperature and pressure, and that it furthermore gives rise to additional physical behavior in the contributions to the electrostatic Helmholtz energy.[22]

The goal of this article is to present a physically sound extension of the Cubic Plus Association (CPA) EoS[27] to handle electrolytes, following the insights obtained from previous publications.[11,22,23] A simple one-parameter scheme is presented to obtain binary interaction parameters for the EoS to accurately represent VLE, LLE, and SLE.

Methods and Parameter Estimation

The e-CPA equation of state

The residual Helmholtz energy A^{r} of the CPA EoS is extended to account for the electrostatic interactions and the Gibbs energy of hydration using the Debye–Hückel[8] and Born[19] models as shown in Eq. 2

$$A^{\mathrm{r}} = A^{\mathrm{SRK}} + A^{\mathrm{assoc}} + A^{\mathrm{DH}} + A^{\mathrm{Born}} \tag{2}$$

The residual Helmholtz energy of the Soave–Redlich–Kwong (SRK) EoS is calculated from Eq. 3

$$\frac{A^{\mathrm{SRK}}}{n_T RT} = -\ln\left(1-\frac{b}{v}\right) - \frac{a(T)}{bRT}\ln\left(1+\frac{b}{v}\right) \tag{3}$$

where n_T is the total mole number, R is the gas constant, T is the temperature, v is the molar volume, b is the covolume parameter of the mixture calculated from a linear mixing rule $b = \sum_i x_i b_i$ of the pure component covolume parameter b_i and the mole fractions of component i (x_i), and $a(T)$ is the temperature-dependent attractive energy of the mixture calculated using the Huron–Vidal infinite pressure mixing rule using Eq. 4, in which a_i is the pure component attractive energy obtained from $a_i(T) = a_{c,i}\left(1+c_{1,i}\left(1-\sqrt{T/T_{c,i}}\right)\right)^2$, where $T_{c,i}$ is the critical temperature, $a_{c,i}$ is the pure component attractive energy at the critical point

$$\frac{a}{b} = \sum_i x_i \frac{a_i}{b_i} - \frac{g^{E,\infty}}{\ln 2} \tag{4}$$

The excess Gibbs energy at infinite pressure $g^{E,\infty}$ is calculated using the modified Huron-Vidal/NRTL equation as shown in Eq. 5

$$\frac{g^{E,\infty}}{RT} = \sum_i x_i \frac{\sum_j x_j b_j \exp\left(-\alpha_{ji}\frac{\Delta U_{ji}}{RT}\right)\frac{\Delta U_{ji}}{RT}}{\sum_j x_j b_j \exp\left(-\alpha_{ji}\frac{\Delta U_{ji}}{RT}\right)} \tag{5}$$

In which α_{ji} is the NRTL nonrandomness parameter and ΔU_{ji} is the change in interaction energy between like and unlike interactions $\Delta U_{ji} = U_{ij} - U_{jj}$. Note that Eq. 5 reduces to the normal quadratic mixing rule (see Eq. 6) for the

Table 2. Conventional Standard State Properties Used in This Work (Adopted from Wagman et al.[44] and Correlated Using the Extended UNIQUAC Heat Capacity Correlation)

	$\Delta_{\mathrm{form}}G$ (kJ/mol)	$\Delta_{\mathrm{form}}H$ (kJ/mol)	C_p^o (J/mol/K) (T in K)
Na^+	−261.9	−240.1	$600.6-1.101T-\frac{23232}{T-200}$
K^+	−283.3	−252.4	$415.1-0.814T-\frac{16316}{T-200}$
Cl^-	−131.2	−167.2	$400.4-1.131T-\frac{18574}{T-200}$
SO_4^-	−744.5	−909.3	$643.3-1.760T-\frac{37903}{T-200}$
NaCl	−384.14	−411.15	50.5
$NaCl{\cdot}2H_2O$	−858.96	−992.45	230.0
KCl	−409.14	−436.74	51.3
Na_2SO_4	−1270.2	−1387.1	128.2
$Na_2SO_4{\cdot}10H_2O$	−3646.8	−4327.3	492.3
K_2SO_4	−1321.4	−1437.8	131.5

Table 3. Summary of Parameter Estimation and Modeling Results for 54 salts: C_i is the Peneloux Parameter, see Discussion Section, Eq. 30

Salt	ΔU_{sw}/R @ 25°C (K)	A (K)	T_α (K)	c_i (cm^3/mol)	T-range (K)	m_{max} (mol/kg)	RAD Δ_{hyd}H (%)	RAD (Φ) (%)	RAD ($\gamma^{\pm}$) (%)	AAD (V^{app}) (cm^3/mol)
NaF	−167.0	−2183	320	−52.2	269–308	1	0.1	1.0	2.2	0.6
KF	−234.7	−983	320	−51.4	251–357	6.5	0.3	1.7	1.5	0.9
RbF	−258.6	–	320	−55.7	298.15	3.5	0.3	0.9	2.6	0.3
CsF	−285.9	–	320	−55.8	298.15	3.5	0.2	0.6	0.9	0.3
HCl	−403.3	−1588	340	−28.8	240–548	6	1.2	1.1	2.7	0.7
LiCl	−440.6	1853	340	−44.9	240–523	6	1.2	3.0	5.7	0.4
NaCl	−223.5	1573	340	−53.5	261–523	6	1.0	1.4	2.4	1.0
KCl	−130.0	1361	340	−58.8	262–550	6	0.6	1.4	3.1	1.9
RbCl	−136.2	1087	340	−58.0	262–318	6	0.5	0.8	1.8	0.5
CsCl	−120.9	938.9	340	−60.0	263–523	6	0.8	1.4	3.6	1.3
$MgCl_2$	−459.6	2439	340	−43.0	240–523	2	0.1	4.7	13	1.4
$CaCl_2$	−380.8	2778	340	−45.3	240–473	3	0.5	5.2	5.1	3.3
$SrCl_2$	−315.3	2260	340	−44.7	258–523	3	0.2	4.6	5.9	7.0
$BaCl_2$	−166.7	1226	300	−53.2	265–523	3	0.4	2.3	8.9	3.8
HBr	−483.3	1435	350	−32.2	273–398	6	0.7	5.6	3.8	0.2
LiBr	−477.4	1311	350	−48.3	240–523	6	0.9	5.3	7.5	0.3
NaBr	−280.3	1322	350	−56.7	246–523	6	0.1	2.4	7.6	0.9
KBr	−162.8	1047	350	−62.5	260–523	6	0.3	1.7	4.9	0.3
CsBr	−133.3	673.1	350	−65.2	273–523	5.7	0.1	2.2	5.0	0.2
$MgBr_2$	−526.2	1802	350	−44.7	240–323	2	0.1	3.7	9.5	0.5
$CaBr_2$	−379.8	627.3	350	−47.6	240–473	3	0.2	4.3	15	2.7
$SrBr_2$	−350.4	401.8	350	−51.5	251–318	2	1.0	3.3	4.6	6.3
$BaBr_2$	−253.6	−296	350	−56.8	250–318	2	0.3	3.0	3.2	1.1
HI	−441.2	–	360	−36.6	298.15	6	0.4	2.4	3.8	0.2
LiI	−403.7	3903	360	−54.3	240–343	3	2.0	1.9	1.5	0.1
NaI	−308.6	849.7	360	−62.2	241–363	6	0.9	3.4	5.7	0.2
KI	−197.8	1224	360	−68.2	255–323	6	2.8	1.1	2.0	0.6
CsI	−113.8	1648	360	−71.0	278–303	3.6	5.6	1.3	3.5	0.2
MgI_2	−480.0	–	360	−51.3	240–298	2	0.3	3.6	4.3	0.1
CaI_2	−419.5	−1403	360	−56.2	240–298	2	1.8	3.2	5.7	0.5
SrI_2	−376.2	–	360	−58.0	264–298	2	0.6	3.7	4.3	0.3
BaI_2	−331.3	–	360	−61.6	240–298	2	1.3	3.1	3.5	0.7
H_2SO_4	558.7	−7431	300	−56.1	253–323	2	1.6	14	42	0.9
Li_2SO_4	−6.36	1961	300	−92.5	250–498	2	0.2	2.1	3.4	1.7
Na_2SO_4	123.8	1163	300	−106.3	272–498	2	0.2	1.7	3.5	2.5
K_2SO_4	77.38	891.5	300	−113	271–498	2	0.3	1.4	2.9	0.4
Rb_2SO_4	23.80	673.9	300	−112	298–323	2	0.2	2.2	1.9	0.9
Cs_2SO_4	−17.71	579.2	300	−119	298–498	2	0.7	0.8	1.5	0.8
$MgSO_4$	118.9	2470	300	−87.9	268–448	4	0.5	7.7	7.8	2.0
$CaSO_4$	–	–	300	–	273–298	0.015	0.3	6.8	6.4	–
LiOH	56.26	2659	273	−47.2	255–523	6	0.9	1.7	2.9	0.8
NaOH	−299.7	1209	273	−48.6	245–523	6	0.1	1.8	4.1	2.8
KOH	−382.3	1145	273	−54.2	240–523	6	0.9	1.8	5.7	0.7
CsOH	−326.4	443.7	273	−58.9	273–523	5.9	0.1	2.0	6.0	0.2
HNO_3	−270.6	−745.0	340	−19.9	265–393	6	0.2	2.0	4.0	1.5
$LiNO_3$	−366.9	−2059	340	−34.3	269–523	6	0.2	3.8	3.2	0.3
$NaNO_3$	−40.88	846.0	340	−43.2	255–373	6	0.2	2.1	3.7	0.9
KNO_3	48.41	445.8	340	−50.5	270–348	6	1.1	2.9	0.4	0.7
$RbNO_3$	36.02	–	340	−49.9	298.15	4.5	1.3	0.7	1.2	0.1
$CsNO_3$	53.91	500.1	340	−53.9	278–323	3.3	0.9	1.5	0.9	0.1
$Mg(NO_3)_2$	−428.0	524.6	340	−31.0	241–323	2	0.7	2.7	7.9	2.5
$Ca(NO_3)_2$	−187.8	1624	340	−35.7	243–424	2	0.8	3.5	9.4	2.0
$Sr(NO_3)_2$	−36.88	–	340	−40.1	266–318	2	1.7	3.6	7.2	0.8
$Ba(NO_3)_2$	52.11	–	340	−46.2	273–318	0.4	2.4	3.1	3.1	0.8
Average	–	–	–	–	–	–	0.8	3.1	5.3	1.2

special case where $\alpha_{ji} = \alpha_{ij} = 0$, $\frac{\Delta U_{ji}}{\ln 2} = \left(\frac{2a_i}{b_i} - \frac{a_{ji}}{b_j}\right)$, and $a_{ij} = \sqrt{a_i a_j}\left(1 - k_{ij}\right)$

$$a(T) = \sum_i \sum_j x_i x_j \sqrt{a_i a_j}\left(1 - k_{ij}\right) \tag{6}$$

In CPA, the pure component parameters $\Gamma_i = a_{c,i}/Rb_i$, b_i, and $c_{1,i}$ are typically estimated using the pure component vapor pressure and liquid density. The binary interaction parameter k_{ij} is adjusted to VLE/LLE data for binary mixtures, or set to 0 for pure predictions. While the quadratic mixing rules given by Eq. 6 are normally used together with CPA, it requires knowledge of the pure component parameters. Since data on pure component vapor pressures/liquid densities do not exist in the case of most strong electrolytes, the parameters are always fitted to binary data—for example, from mixtures of NaCl and water. To reflect this in the parameterization, it was therefore decided to fit the binary interaction energies directly through the Huron–Vidal/NRTL mixing rule in Eq. 5. In the case of ions, we decided to neglect attractive interactions between ions by assuming $\Delta U_{ij} = 0$. The co-volume is furthermore calculated from the ion diameter using Eq. 7

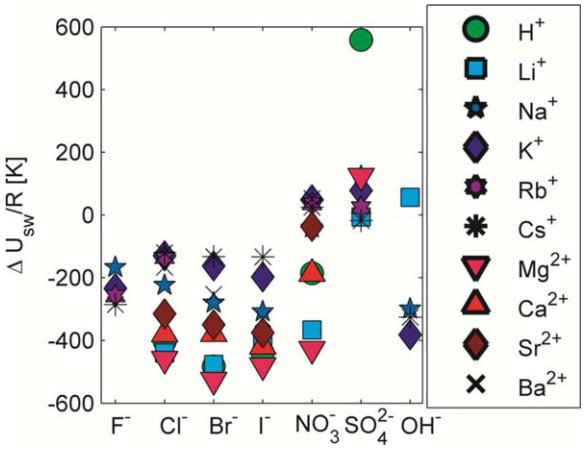

Figure 3. Parameter trend for ion-solvent interaction parameter at 25°C from Table 3.

[Color figure can be viewed in the online issue, which is available at wileyonlinelibrary.com.]

$$b_i = \frac{2}{3} N_A \pi d_i^3 \tag{7}$$

where d_i is the hard-sphere diameter of the ion as obtained from Marcus and shown in Table 1.[28]

The residual Helmholtz energy from the association is calculated from the solution to the constrained optimization problem given by Eq. 8[29–31]

$$\begin{aligned} \min_{\mathbf{X}} \frac{A^{\text{assoc}}}{RT} &= \sum_i n_i \sum_{A \in i} \left(\ln X_{A_i} - \frac{1}{2} X_{A_i} + \frac{1}{2} \right) \\ s.t. \frac{1}{X_{A_i}} &= 1 + \sum_j \rho_j \sum_{B \in j} X_{B_j} \Delta_{A_i B_j} \end{aligned} \tag{8}$$

In Eq. 8 ρ_i is the density of component i, X_{A_i} is the fraction site A on component i that is not bonded to any other site (which are solved following the procedure from Michelsen,[30,31]) and $\Delta_{A_i B_j}$ is the association strength (equilibrium constant), which in CPA is calculated from Eq. 9

$$\Delta_{A_i B_j} = g(\rho) v_{A_i B_j} \left[\exp\left(\frac{\varepsilon_{A_i B_j}}{k_B T} \right) - 1 \right] \tag{9}$$

In Eq. 9, $v_{A_i B_j}$ is the association volume, $\varepsilon_{A_i B_j}$ the association energy, and $g(\rho)$ the radial distribution function. In the case of CPA $g(\rho)$ is approximated by $g(\rho) = (1 - 1.9\eta)^{-1}$ where the packing factor η is given by $b/4v$.

The contribution to the Helmholtz energy from ion-ion interactions is calculated using the expression for the residual Helmholtz energy from Debye and Hückel,[8] as shown in Eq. 10[11]

$$A^{\text{DH}} = -\frac{k_B T V}{4\pi N_A \sum_i n_i z_i^2} \sum_i n_i z_i^2 \chi_i \tag{10}$$

In Eq. 10, V is the total volume, N_A is the Avogadro number, z_i is the charge of component i, and the function χ_i is given by Eq. 11

$$\chi_i = \frac{1}{d_i^3} \left[\ln(1 + \kappa d_i) - \kappa d_i + \frac{1}{2} (\kappa d_i)^2 \right] \tag{11}$$

In Eq. 11, where κ is the inverse Debye screening length, we assume the same value of the ion diameter as in Eq. 7, that is, the same value is used in both the physical part and in the Debye–Hückel part of the EoS.

Finally, the contribution from the Born[19] model is obtained from Eq. 12[20]

$$A^{Born} = \frac{N_A e^2}{8\pi\varepsilon_0} \sum_i \frac{n_i z_i^2}{R_{Born,i}} \left(\frac{1}{\varepsilon_r} - 1 \right) \tag{12}$$

In which $R_{\text{Born},i}$ is the radius of the Born cavity caused by the transfer from vacuum to the fluid phase.

The static permittivity ε_r in A^{DH} and A^{Born} is obtained from known fluid conditions using Eq. 13[23]

$$\frac{(2\varepsilon_r + \varepsilon_\infty)(\varepsilon_r - \varepsilon_\infty)}{\varepsilon_r} = \left(\frac{\varepsilon_\infty + 2}{3} \right)^2 \frac{N_A}{\varepsilon_0 k_B T v} \sum_i x_i g_i \mu_{i,0}^2 \tag{13}$$

In Eq. 13, the infinite frequency permittivity ε_∞ is obtained from the Clausius–Mossotti equation, and the Kirkwood g-factor is obtained from Eq. 14

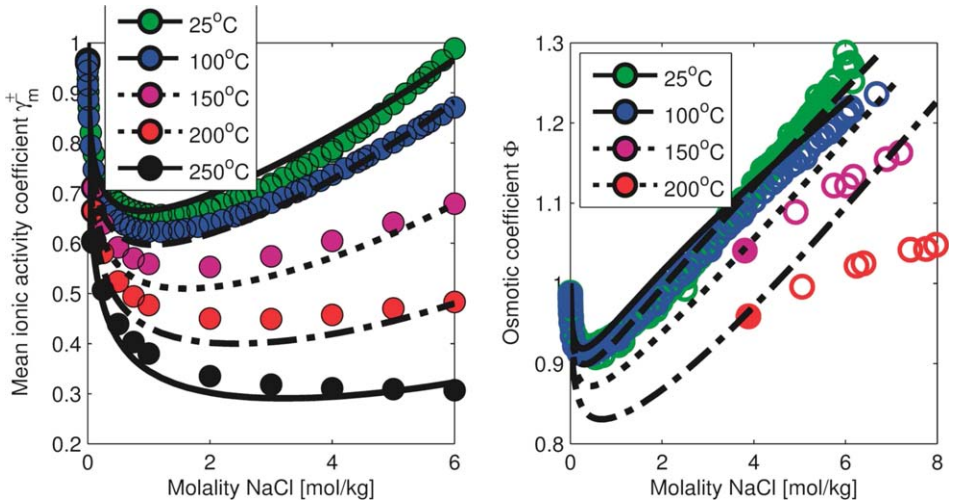

Figure 4. Temperature and concentration dependence of NaCl activity coefficients (left) and osmotic coefficients (right) at bubble point pressure compared to experimental data from the CERE Electrolyte Database.[47]

[Color figure can be viewed in the online issue, which is available at wileyonlinelibrary.com.]

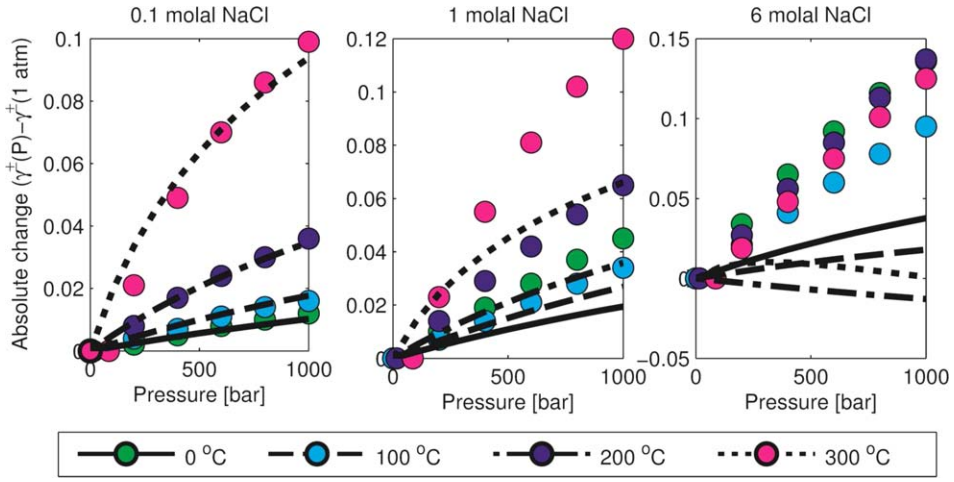

Figure 5. Effect of pressure on activity coefficients of NaCl as a function of pressure, temperature, and concentration with e-CPA (lines) in comparison to the results with the detailed model by Pitzer et al.[48] (circles).

[Color figure can be viewed in the online issue, which is available at wileyonlinelibrary.com.]

$$g_i = 1 + \sum_j \frac{z_{ij} P_{ij} \cos\gamma_{ij}}{P_i \cos\theta_{ij} + 1} \frac{\mu_{0,j}}{\mu_{0,i}} \tag{14}$$

In Eq. 14, z_{ij} is the coordination number of molecule j around a central molecule i, P_{ij} is the probability that molecule i is associated to molecule j (which is determined from the solution to the site fractions X_{A_i}), $\mu_{i,0}$ is the vacuum dipole moment of molecule i, the angle $\cos\gamma_{ij}$ corresponds to the angle between the dipole moments of molecule i and j in the hydrogen bond network. Maribo-Mogensen et al.[23] provide more details and parameter values used in this study.

The presented model requires a binary interaction parameter between each ion in the modeled mixture, the Huron–Vidal/NRTL interaction energy, which is assumed to be symmetrical, that is, $\Delta U_{ij} = \Delta U_{ji}$. The ion-ion interaction parameter and the NRTL nonrandomness parameter are defined as zero to obtain a simple mixing rule for the excess energy from Eq. 5 which is now simplified as shown in Eq. 15

$$\frac{g^{E,\infty}_{\text{ions}}}{RT} = \frac{1}{b} \sum_i \sum_j x_i x_j b_j \frac{\Delta U_{ji}}{RT} \tag{15}$$

Note that the simple form from Eq. 15 makes it possible to obtain salt-specific parameters for the salt s and neutral molecule i, ΔU_{si}, that are related to the ion-specific parameters through Eq. 16

$$\frac{\Delta U_{si}}{RT} = \sum_{j \in s}^{\text{ions}} \frac{v_j (b_j + b_i)}{v_s b_i + b_s} \frac{\Delta U_{ji}}{RT} \tag{16}$$

In Eq. 16, v_i is the stoichiometric number of ion i per salt molecule s, v_s is the total stoichiometric number of dissociated molecules in salt s, $\sum_{j \in s} v_j$, and b_s is the covolume parameter of the salt $\sum_{j \in s} v_j b_j$.

Parameter estimation

The electrolyte CPA (e-CPA) model presented above has several parameters, some of which can be estimated from literature data, others from solubility information, while for others some assumptions are needed. Moreover, there are more than one way to estimate the parameters and whereas the approach we used is presented below, alternative methods will be mentioned in the discussion section.

We start with $R_{\text{Born},i}$, that is, the radius of the Born cavity. In literature many approaches for defining the effective hydration radius have been suggested. Some researchers adopt the diameter ("distance of closest approach") from the Debye–Hückel term,[32,33] while others use adjusted hydrated diameters,[20,21,34–41] where the ion diameters are typically slightly increased (compared to the hard-sphere diameter σ), presumably due to the effect of hydration. Only Myers

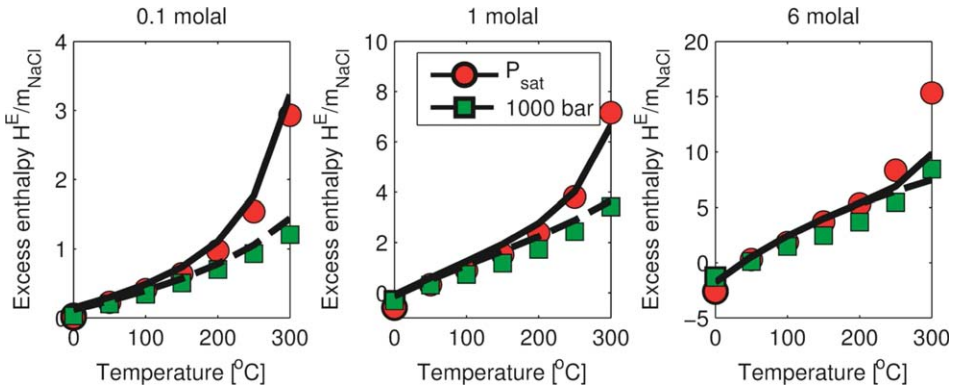

Figure 6. Excess enthalpy of NaCl calculated with the e-CPA model and with the detailed model from Pitzer et al.[48]

[Color figure can be viewed in the online issue, which is available at wileyonlinelibrary.com.]

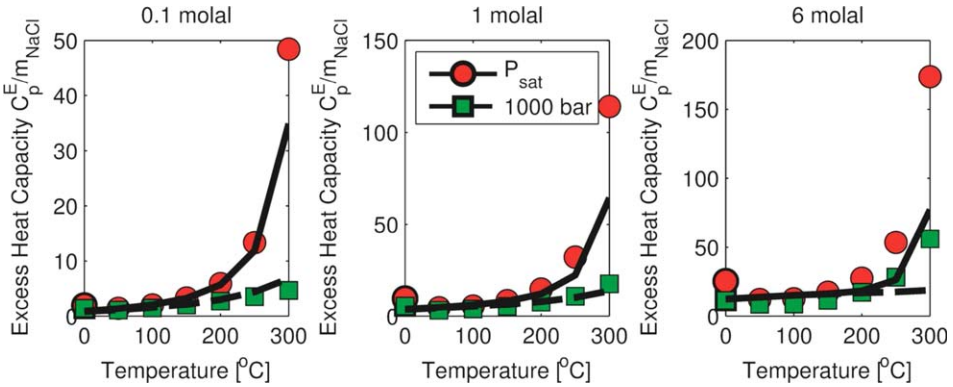

Figure 7. Excess heat capacity of NaCl calculated with the e-CPA model and with the detailed model from Pitzer et al.[48]

[Color figure can be viewed in the online issue, which is available at wileyonlinelibrary.com.]

et al.[20] and Herzog et al.[10] performed comparisons of calculated values to experimental values of the Gibbs energy of hydration at 25°C and both showed large deviations. While there are multiple sources giving rise to the hydration free energy, the Born term is by far the most important contribution.[42] Marcus[42] calculated the hydration free energy from the entropy and enthalpy of hydration at 298.15K. As the Born term is an internal energy contribution, it was decided to fit the Born radii of the ions to data for the enthalpy of hydration at 25°C. To calculate the enthalpy of hydration, one needs the ideal gas formation enthalpies as well as the absolute enthalpy of hydration of the H^+ ion, where we adopt the recent value of 1150.1 kJ/mol from Mejias and Lago.[43] The conventional aqueous standard state enthalpy of formation of the salts are obtained from Wagman et al.,[44] and the absolute enthalpy of formation may then be determined using Eq. 17

$$\Delta_f H(i,aq,abs) = \Delta_f H(i,aq,conv) + z\Delta_f H\left(H^+,aq,abs\right) \quad (17)$$

The hydration enthalpy is then determined by subtracting the enthalpy of formation for the ideal gas ions (using the values from Table 1)

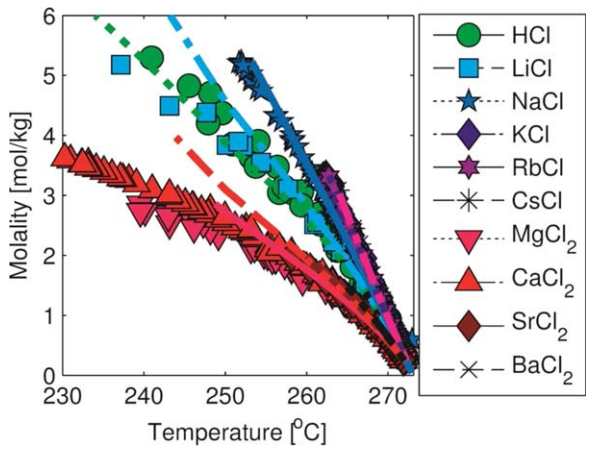

Figure 8. Experimental freezing point depression data for chloride salts at 1 atm in comparison with results from the e-CPA model. Data from the CERE Electrolyte Database.[47]

[Color figure can be viewed in the online issue, which is available at wileyonlinelibrary.com.]

$$\Delta_{hyd}H(i) = \Delta_f H(i,aq,abs) - \Delta_f H(i,g,abs) \quad (18)$$

To calculate a salt-specific parameter, the ion-specific parameters must first be specified for the system. The enthalpy of hydration is then calculated using e-CPA from Eq. 19, and the Born radii of the ions are varied to obtain the best match of the hydration enthalpy of the salt. This leads to the ion-specific parameters shown in Table 1

$$\Delta_{hyd}H = \lim_{n_i\to 0}\left[H_i^{liq} - H_i^{ig}\right] = \lim_{n_i\to 0}\left[-RT^2\left(\frac{\partial \ln\varphi_i^l}{\partial T}\right)_P\right] \quad (19)$$

The second set of parameters that are needed are the interaction energies between salts (or ions) and the solvents (e.g., water) which appear in Eqs. 5, 15 and 16. At this stage, one should choose whether to proceed with salt-specific or ion-specific parameters.

One of the challenging tasks in dealing with modeling of electrolyte mixtures is how to obtain ion-specific parameters. This requires simultaneous regression of many different parameters to all available experimental data. Yet, not every ion is equally well described, and the data becomes increasingly scarce for all other solvents than water. Therefore, to provide a model that is simple to apply to, for example, determination of gas solubility in mixed solvents, we propose (as a first approximation) to determine salt-specific parameters obtained from various sources (e.g., through SLE, and VLE data for the pure salt) and use this parameter to predict the behavior at other conditions and in salt mixtures.

The ion-specific parameters must be calculated from the salt-specific parameter to perform EoS calculations. These parameters can only be determined exactly, if the degree of freedom is zero. Therefore, the parameterization of a pure salt requires an extra thermodynamic condition, such as equating the contribution from the anion and cation, $\Delta U_{ai} = \Delta U_{ci}$ or $v_a(b_a+b_i)\Delta U_{ai} = v_c(b_c+b_i)\Delta U_{ci}$, neglecting the anion or the cation interactions $\Delta U_{ai} = 0 \vee \Delta U_{ci} = 0$, or something similar. Such extra thermodynamic conditions have also previously been applied to obtain ion-specific parameters using, for example, the Extended UNIQUAC model by Thomsen et al.,[45] in which the interaction parameters for the hydrogen ion are set to zero. The salt-water interaction parameter does not depend on the extra thermodynamic condition used to parameterize the salt, and it is evident from Figure 2 that the model can successfully correlate the osmotic and activity coefficients

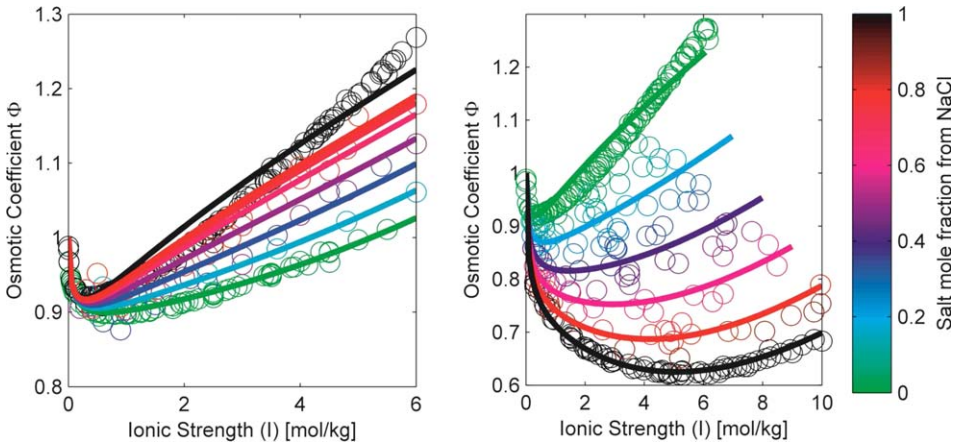

Figure 9. Osmotic coefficients in mixtures of KCl + NaCl (left) against data from Saad et al.[49] and Na_2SO_4 + NaCl (right) at 25°C, 1 atm against data from Rard et al.[50]

[Color figure can be viewed in the online issue, which is available at wileyonlinelibrary.com.]

of NaCl at 25°C by adjusting only the salt-water interaction parameter, ΔU_{sw} once the Rborn has been fixed. More details on the parameter estimation (objective function, etc.) are provided in "Parameterization and Model Validation" section.

For simple binary mixtures, salt-specific parameters are adequate, but when dealing with mixtures containing multiple ionic species, the system becomes over-specified, indicating that parameters must be defined from a subset of the possible salts, or from a least-squares type regression of the ion-solvent interaction parameters.

Improvements for the density require inclusion of the volume translation, which is discussed in the Discussion section.

Temperature Dependence of Salt-Water Interaction Parameters

The temperature dependence of the physical properties of electrolytes mixtures has been investigated by several groups during the past 40 years through, for example, calorimetric measurements and modeling. At infinite dilution, a nonmonotonic behavior of the apparent molal heat capacity is observed. Cobble et al.[46] ascribed the nonmonotonic behavior of the standard state heat capacity to the structure- and field behavior of electrolytes, in which it is suggested that the structural interactions dominate the ion-solvent interactions at low temperatures, whereas it is the electrical field that dominates at high concentrations.

By adjusting the salt-water interaction parameter at different temperatures independently to temperature-dependent osmotic and activity coefficient data, it was found that the temperature dependence of ΔU_{ws} follows the nonmonotonic functional form shown in Eq. 20

$$\Delta U_{ws}/R = \Delta U_{ws}^{\mathrm{ref}}/R + \alpha_i \left[\left(1 - \frac{T}{T_\alpha}\right)^2 - \left(1 - \frac{T_{\mathrm{ref}}}{T_\alpha}\right)^2 \right] \quad (20)$$

In which $\Delta U_{ws}^{\mathrm{ref}}$ is the binary interaction parameter at the reference temperature $T_{\mathrm{ref}} = 298.15\mathrm{K}$, and both the crossover temperature $T_{a,i}$ and linear dependency α_i can be adjusted to match the experimental data as shown for NaCl in Figure 4.

The Role of Solid-Liquid Equilibrium Data

A large amount of experimental data exists for osmotic coefficients or water activities in aqueous salt mixtures at 25°C, and for many salts satisfactory amount of temperature-dependent data are also available. The situation is different

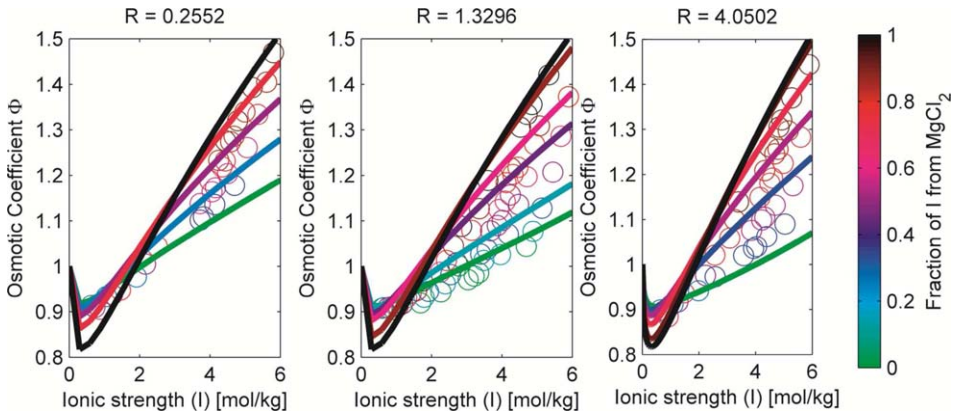

Figure 10. Osmotic coefficients of ternary salt mixtures (NaCl, KCl, and $MgCl_2$) at 25°C, 1 atm against data from Saad et al.[49]

[Color figure can be viewed in the online issue, which is available at wileyonlinelibrary.com.]

Table 4. CPA Parameters for Selected Compounds[2,27,51]

Component	T_c	b	$\Gamma = \frac{a_0}{Rb}$	c_1	v_{A_i,B_j}	$\frac{\varepsilon_{A_i,B_j}}{k_B}$	Association scheme
Unit	(K)	$\frac{\text{cm}^3}{\text{mol}}$	(K)		$\frac{\text{cm}^3}{\text{mol}}$	K	
Water	647.13	14.52	1017.3	0.6736	1.004	2003.25	4C
Methanol	512.64	30.98	1573.7	0.4310	0.499	2957.78	2B
Ethanol	513.92	49.11	2123.8	0.7369	0.393	2589.85	2B
1-Propanol	536.78	64.11	2234.5	0.9171	0.519	2525.86	2B
Ethylene Glycol	563.05	79.70	2368.6	0.9784	0.654	2525.86	2B
Pentane	469.7	91.01	2405.1	0.7986	–	–	–
Benzene	562.16	74.99	2867.2	0.7576	–	–	1 negative site
Toluene	591.8	92.14	3051.4	0.8037	–	–	1 negative site
Methane	190.6	29.1	959.03	0.4472	–	–	–
Carbon Dioxide	304.21	27.20	1551.2	0.7602	–	–	–

in the case of mixed solvents, where this type of data is scarce. However, even for mixed solvent cases a considerable amount of solid-liquid equilibrium data exists, and by extending the model to handle the solid-liquid equilibrium in water-salt mixtures it becomes possible to use the SLE-data in mixed solvent-cases also for parameter estimation. The model for the fugacity of solid ice is given by Eq. 21

$$\ln\gamma_w x_w = -\frac{\Delta_{\text{fus}}H}{RT}\left(1-\frac{T}{T_{\text{tri}}}\right)-\frac{\Delta C_{p,i}}{R}\left(1-\frac{T_{\text{tri}}}{T}-\ln\frac{T_{\text{tri}}}{T}\right) \quad (21)$$

In which $T_{\text{tri}} = 273.16\text{K}$, $\Delta_{\text{fus}}H = 6001.74\frac{\text{J}}{\text{mol}}$, and $\Delta C_{p,i} = 38.03\frac{\text{J}}{\text{mol}\times\text{K}}$. While Eq. 21 is a good approximation for extrapolation of normal compounds around their triple point, the triple point of pure salts is too high compared to the temperature region of interest (e.g., 250–400K) in which precipitation of salt from supersaturated solutions is observed. As the standard state properties are not sufficiently accurate for a solid-liquid equilibrium calculation, it is necessary to use the activity coefficients and standard state properties to determine the SLE of salts using Eq. 22

$$\text{In}\,K_j = RT\sum_i \nu_{i,j}\ln a_i \quad (22)$$

Activity coefficient models for electrolyte mixtures, such as the Extended UNIQUAC,[45] adjust the standard state properties to fit the solid-liquid equilibrium constants. The standard state properties used in this work are summarized in Table 2.

Parameterization and model validation

General – Activity Coefficients. Using the model presented in the previous sections (and considering also the discussions shown in detail in the Discussion section) it was decided to neglect ion-solvent association and regress the salt-water model parameter ΔU_{sw} to osmotic and activity coefficient data up to the concentration indicated in Table 3 (or the solubility limit of the salt). The objective function is given by Eq. 23 (note that the model gives higher weight to osmotic coefficient data at higher concentrations)

Table 5. Binary Interaction Parameters Used for Mixtures with Water

Binary mixture	Water-Methanol	Water-Ethanol	Water-1-Propanol	Water-Ethylene Glycol
k_{ij}	−0.09	−0.11	−0.08	−0.115

$$R = \sum_i \left(\frac{\gamma^{\pm}_{\text{exp}}-\gamma^{\pm}_{\text{calc}}}{\gamma^{\pm}_{\text{exp}}}\right)^2 + \sum_i m_i\left(\frac{\phi_{\text{exp}}-\phi_{\text{calc}}}{\phi_{\text{exp}}}\right)^2 \quad (23)$$

Where m_i is the salt molality. The parameters are summarized in Table 3 along with results for the deviations in the osmotic coefficient and the mean ionic activity coefficient at 25°C using the recommended diameter values from Table 1. Results are reported as RAD (the relative average deviation $\text{RAD} = \frac{1}{N}\sum_i^N \left|\frac{x_i^{\text{exp}}-x_i^{\text{calc}}}{x_i^{\text{exp}}}\right|$) and AAD (the absolute average deviation is defined as $\text{AAD} = \frac{1}{N}\sum_i^N \left|x_i^{\text{exp}}-x_i^{\text{calc}}\right|$).

Excellent agreement is obtained for most salts up to the solubility limit.

Figure 3 visualizes the parameter trends of ΔU_{sw} at 25°C for the salt-water interaction parameter for all cations and anions. It is evident from the parameter trends shown in Figure 3 that the salts H_2SO_4, $LiNO_3$, $Mg(NO_3)_2$, LiOH, $BaBr_2$ fall outside the parameter trends. At least in the case of H_2SO_4, this can most likely be ascribed to the assumption of complete dissociation being incorrect, making H_2SO_4 behave as a 1:1 salt rather than a 2:1 salt due to the chemical equilibrium leading to formation of the HSO_4^- ion. Furthermore, Figure 3 shows that it may be possible to get reasonable ion-specific parameters for certain ion combinations with the presented model, whereas other trends could only be captured by introducing ion-ion interaction parameters. Rather than introducing additional parameters to allow fitting of ion-specific parameters for the full set, this work focuses on validating the model for a variety of applications. Validations and further applications are shown in section "Predictions with e-CPA."

Figure 4 shows how the model captures the temperature dependence of the activity coefficients of NaCl in comparison to experimental data. Figure 5 shows that the pressure dependence of the model is similar to the detailed Pitzer model[48] at 0.1 and 1.0 molal, whereas the e-CPA and the Pitzer models disagree on the pressure dependence at high concentrations. Although there is no available experimental data (to the best of our knowledge), it should be noted that the pressure-dependence of e-CPA may be incorrect at high concentrations due to the problematic representation of the density in the absence of a Peneloux volume correction (see Discussion section).

The e-CPA and the detailed Pitzer model also agree on the excess enthalpy at the saturation pressure and at 1000 bar as evidenced by Figure 6 using the apparent molal excess enthalpy which can be calculated from Eq. 24

Table 6. Estimated Binary Interaction Parameters of Salts with Different Solvents at 25°C

$\Delta U_{sa}/R$ (K)	NaCl	NaBr	KCl	Na_2SO_4	K_2SO_4
Methanol	322.4	219.6	567.5	1165	941.2
Ethanol	372.6	–	522.6	–	–
Propan-1-ol	580.1	–	–	–	–
Ethylene glycol	−100	–	100.0	–	–

$$\Delta H^E = -\frac{RT^2}{m_{\text{salt}}}\sum_i n_i\left(\frac{\partial \ln\gamma_i}{\partial T}\right) \tag{24}$$

The specific excess heat capacity is determined from the temperature derivative of Eq. 24 and it can be seen in Figure 7 that good agreement with the pressure and temperature dependence of the excess heat capacity is obtained.

Validation for Freezing Point Depression. The freezing point depression can be evaluated using Eq. 21. The results for chloride salts with the e-CPA model are presented in Figure 8, indicating that the model provides a reasonable agreement with the freezing point data down to 245K, whereas the agreement is generally less satisfactory at lower temperatures. At lower temperatures, the ion-water association becomes stronger, and the inclusion of an explicit term to account for this association may therefore improve the results at the lower temperatures.

Validation for Mixed Salts. While the parameters presented in Table 3 are salt-specific, they may be applied to mixed salt solutions, provided that the anion and cations are compatible. It is therefore possible to mix NaCl and Na_2SO_4 or NaCl, KCl, and $MgCl_2$, whereas a mixture of NaCl and K_2SO_4 will likely yield problematic results due to the opposite trends in the salt-specific parameters for the anions and cations, as seen in Figure 3. While ion-specific parameters could still be fitted to this system, additional parameters such as the ion covolume parameter should be adjusted or it could be necessary to introduce cation-anion interaction parameters. Representative results for osmotic coefficients are shown in Figure 9 indicating that the parameters optimized for the pure salts, can be used to predict the results of the mixtures. This observation also holds true for the mixture of NaCl + KCl + $MgCl_2$ shown in Figure 10. Reasonably good predictions are obtained in all cases.

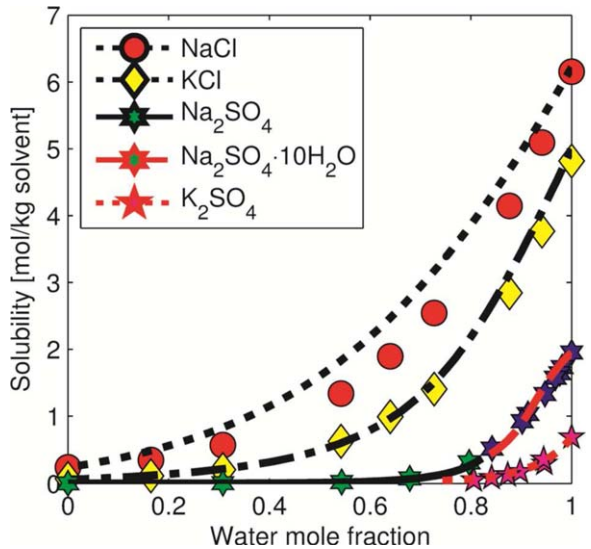

Figure 11. Solubility of different salts in water + methanol using the binary interaction coefficients shown in Table 6.

Data from Pinho and Macedo[52] and Emons and Röser[53] at 25°C, 1 atm. [Color figure can be viewed in the online issue, which is available at wileyonlinelibrary.com.]

Predictions with e-CPA for a wide range of electrolyte systems

Mixed Solvents. The solubility of salts depends greatly on the solvent, partly due to the change in the static permittivity, which affects the electrostatic interaction energy. In the e-CPA, EoS we determine the static permittivity of the mixed solvent from the model presented by Maribo-Mogensen et al.[23] There are only limited VLE and activity coefficient data available for electrolytes in solvents other than water, and it is therefore suggested to match the salt-solvent interaction coefficient to the salt solubility, provided that the concentration is sufficiently high for this parameter to affect the solubility. The CPA parameters used for the solvents are shown in Table 4 and the binary parameters are shown in Table 5 while the salt-solvent parameters are shown in Table 6.

Results for the solubility of salts in methanol are shown graphically in Figure 11, while Figure 12 shows the solubility of NaCl and KCl in mixtures of water and other solvents. The predicted effect of methanol on the SLE-diagram of NaCl + Na_2SO_4 is shown in Figure 13, indicating that the model has good predictive capabilities, once the binary interaction parameters have been determined from solubility data for the pure salts. It is also evident that the calculated density at the saturation limit becomes less accurate at increasing methanol concentrations, indicating that the differences in the ion-solvent association in different solvents could be important for improving the overall model performance.

Predicted Solubility in Mixed Solvent. The temperature-dependent methanol-NaCl interaction parameters were obtained from fitting to the data from Pinho and Macedo[54] as seen in Figure 14. Using the temperature-dependent NaCl-water and NaCl-methanol interaction parameters, the solubility of NaCl in water and methanol mixtures at elevated temperatures and pressures were predicted, indicating that the model could be suited for application to scaling at reservoir conditions.

Solubility of Nonelectrolytes. The solubility of nonelectrolytes is commonly characterized by the Setschenow coefficients k_{si}^S, defined by Eq. 25

$$k_{si}^S = \lim_{m_S\to 0}\frac{1}{m_S}\log\frac{S_i^o}{S_i} \tag{25}$$

In which m_S is the molality of salt and S_i^o is the solubility in the salt-free solution, whereas S_i is the solubility in the salt-containing solution. By matching the Setschenow coefficients, it is possible to determine the interaction parameters of the salt with the nonelectrolyte as shown in Table 7 and then predict the solubility of nonelectrolytes in water + NaCl as shown in Figure 15. By assuming that the salt-methanol and salt-gas interaction parameters are independent of temperature, it becomes possible to estimate the effect of salts on the solubility of methane and CO_2 in water as shown in Figure 16 and Figure 17, respectively. By

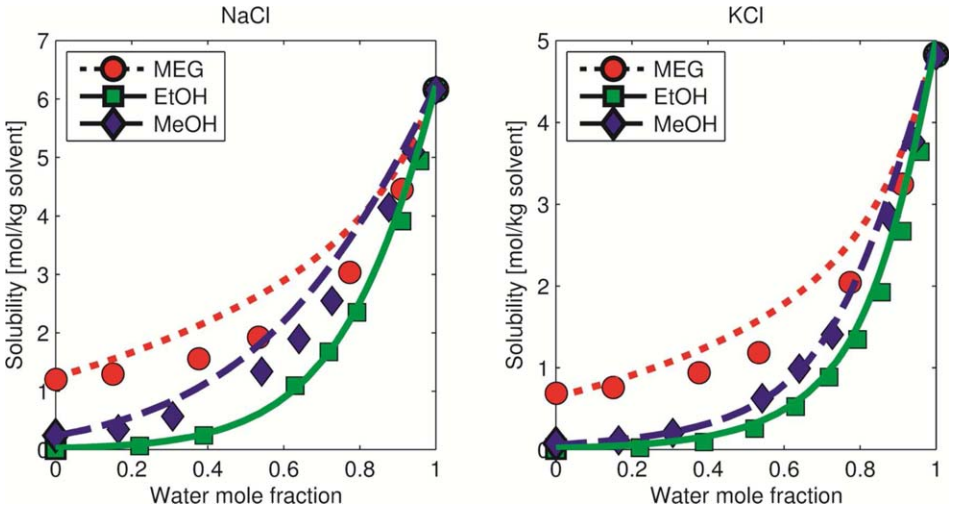

Figure 12. Predicted solubility of NaCl and KCl in mixed solvents with water (ethylene glycol, methanol, and ethanol) at 25°C, 1 atm.

[Color figure can be viewed in the online issue, which is available at wileyonlinelibrary.com.]

furthermore adopting the methanol-salt interaction parameter from Figure 14, the model provides reasonable predictions of the solubility of CO_2 in a mixed solvent containing both water, methanol, and NaCl as shown in Figure 18 where e-CPA slightly over-predicts the solubility, but provides a good qualitative agreement with trends, including precipitation of NaCl.

Salt Effect on Gas Hydrate Formation Pressures. An important application of equations of state is to predict the formation curves for gas hydrates. The presence of salts will typically inhibit gas hydrate formation and it is therefore of interest to see whether the presented model is capable of capturing these trends. The methods and parameters have been presented previously by Karakatsani and Kontogeorgis,[63] and will only be briefly summarized for the case of structure I methane clathrate. The hydrate phase equilibrium is calculated from the Van der Waals and Platteeuw[64] model, where the fugacity of water in the hydrate phase is calculated from Eq. 26

$$f_w^H = f_w^{\mathrm{EH}} \exp\left(\frac{\mu_w^H - \mu_w^{\mathrm{EH}}}{RT}\right) \tag{26}$$

Where the fugacity of water in the empty hydrate f_w^{EH} may be calculated using Eq. 27

$$f_w^{\mathrm{EH}} = P_w^{\mathrm{EH}} \varphi_w^{\mathrm{EH}} \exp\left(\int_{P_w^{\mathrm{EH}}}^{P} \frac{V^{\mathrm{EH}}}{RT} dP\right) \tag{27}$$

In which P_w^{EH} is the vapor pressure of the empty structure I hydrate is calculated from Sloan and Koh[65] and the volume of the hydrate is obtained from the correlation by Avlonitis.[66] The change in the chemical potential from the empty hydrate to the hydrate with methane as a guest molecule is determined from Eq. 28

$$\frac{\mu_w^H - \mu_w^{\mathrm{EH}}}{RT} = v_s \ln\left(1 - \Theta_{\mathrm{CH_4}}^s\right) + v_l \left(1 - \Theta_{\mathrm{CH_4}}^l\right) \tag{28}$$

In which v_s and v_l are the number of cavities per water molecule for the small and large cavities ($v_s = 1/23$ and v_l

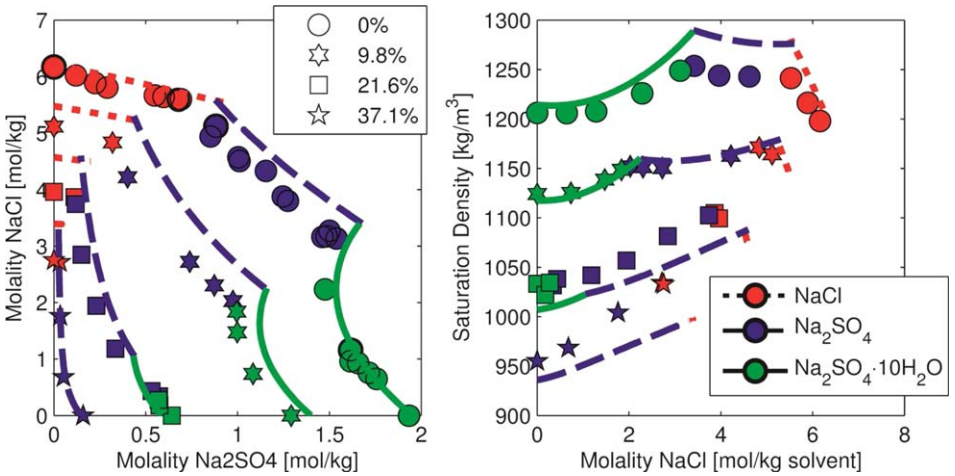

Figure 13. Predicted SLE-diagram of NaCl + Na_2SO_4 at 25°C, 1 atm increasing methanol concentrations from 0 to 37 wt % (left), and the density of the saturated solution, including Peneloux volume correction. Data from Emons and Röser.[53]

[Color figure can be viewed in the online issue, which is available at wileyonlinelibrary.com.]

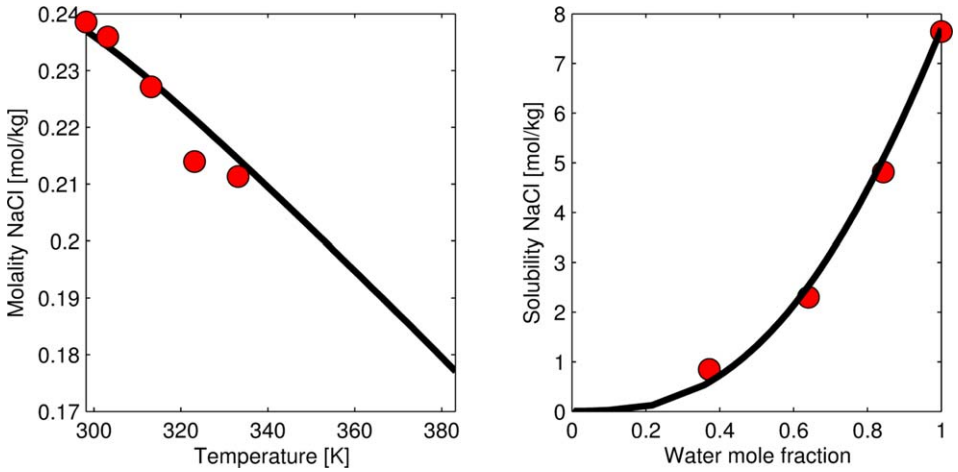

Figure 14. Left: Correlated solubility of NaCl in anhydrous methanol with $\alpha = 950$K and $T_\alpha = 273.15$ at the saturation pressure. Data from Pinho and Macedo.[54] Right: Predicted solubility in water + methanol at 466.2K, 72 bar. Data from Djamali et al.[55]

[Color figure can be viewed in the online issue, which is available at wileyonlinelibrary.com.]

$= 3/23$ for structure I hydrate). The occupancy of the small and large cavities $\Theta^s_{CH_4}$ and $\Theta^l_{CH_4}$ are calculated from the Langmuir-equation from Eq. 29

$$\Theta_{CH_4} = \frac{C_{CH_4} f_{CH_4}}{1 + C_{CH_4} f_{CH_4}} \tag{29}$$

The Langmuir constants for the small and large cavities, C_{CH_4}, are calculated from the simplified procedure by Parrish and Prausnitz.[67] Karakatsani and Kontogeorgis[63] found that the appropriate Langmuir parameters for the structure I methane clathrate using CPA are given by $C^s_{CH_4} = \frac{1}{T}\exp\left(\frac{1970}{T}\right)$ and $C^l_{CH_4} = \frac{0.316}{T}\exp\left(\frac{2048}{T}\right)$. The results are summarized in Figure 19, showing that the e-CPA model provides excellent predictions of the gas hydrate formation pressures, without modifying parameters from the previous work by Karakatsani and Kontogeorgis.[63]

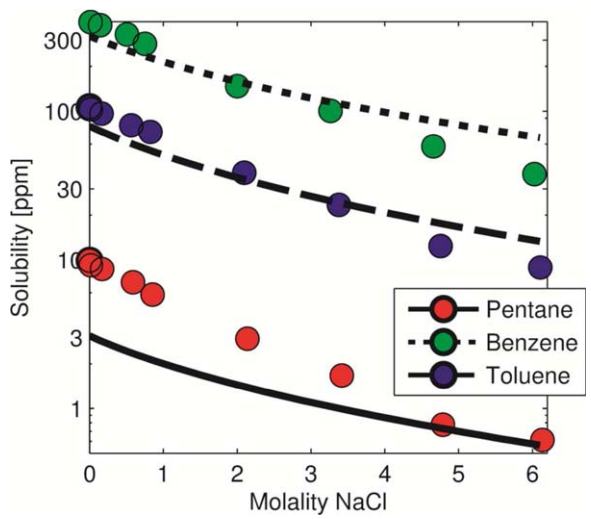

Figure 15. Comparison of predicted solubility of selected nonelectrolytes at 25°C, 1 atm in water + NaCl using e-CPA against experimental data from Price.[58]

Note that the discrepancy observed in the pure solvent is due to the water-solute interaction parameters that have been previously determined from other data sources. [Color figure can be viewed in the online issue, which is available at wileyonlinelibrary.com.]

Discussion

Certain aspects of the e-CPA model we have presented in this work are discussed in more detail here; all these point to future improvements and a more complete implementation of the model. The section is completed with a general overview.

Improvement of the volume predictions

Figure 2 demonstrates that the model can successfully correlate thermodynamic properties of aqueous salt mixtures using only a single parameter at 25°C. However, when the model uses the covolume parameter b_0 calculated from the

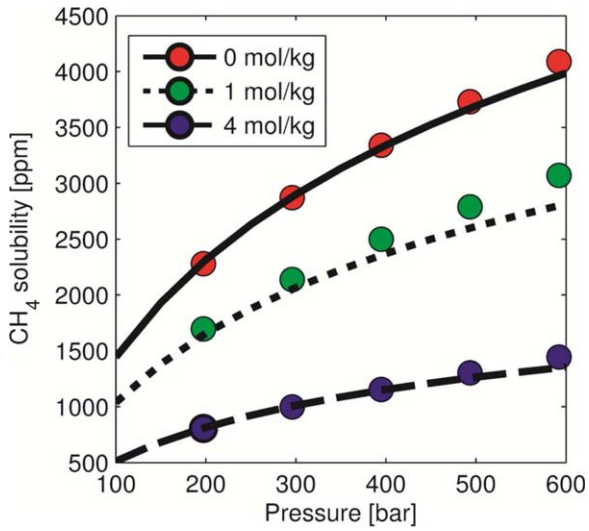

Figure 16. Predicted solubility of methane in water with NaCl at 51.5°C using e-CPA against experimental data from O'Sullivan and Smith.[59]

[Color figure can be viewed in the online issue, which is available at wileyonlinelibrary.com.]

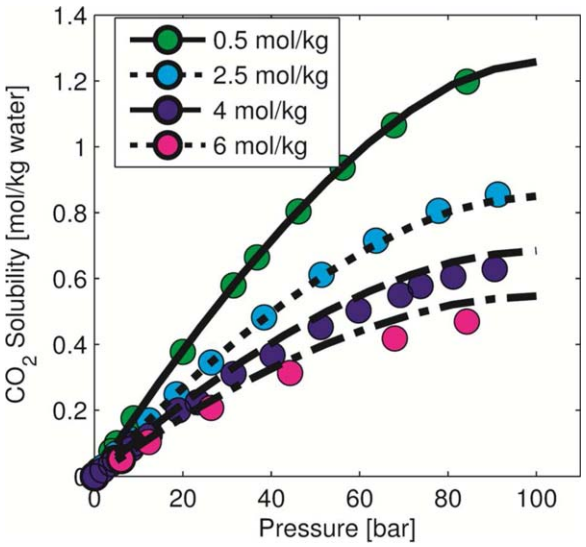

Figure 17. Predicted solubility of CO_2 in water with NaCl at 40°C using e-CPA against experimental data from Rumpf et al.[60] and Kiepe et al.[61]

[Color figure can be viewed in the online issue, which is available at wileyonlinelibrary.com.]

ion diameters the apparent molar volume is over-estimated by about three times. Figure 20 shows the optimal deviations from experimental data when the ΔU_{sw} parameter is optimized to osmotic and activity coefficient data, indicating that the covolume parameter for NaCl in the present model should be changed from 57.32 to 16.83 cm^3/mol to simultaneously capture volumetric and thermodynamic (activity coefficient) data with a satisfactory accuracy.

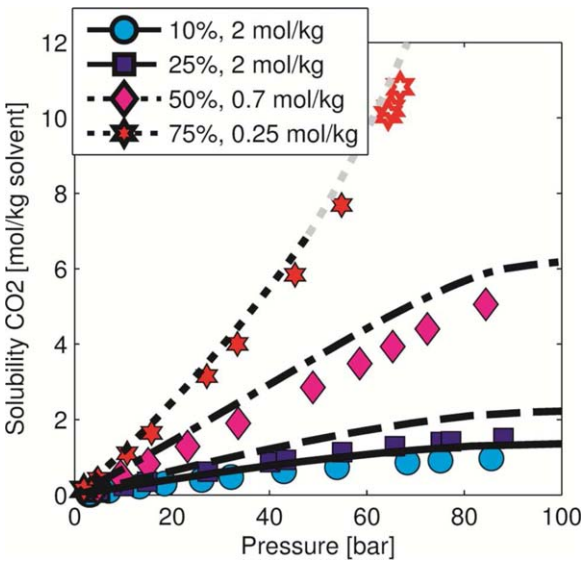

Figure 18. Predicted solubility of CO_2 at 40.5°C using e-CPA in a mixed solvent containing water and methanol (wt %) with different molalities of NaCl (mol/kg solvent) using $k_{ij} = 0.0266$ for the CO_2-methanol binary.

Grey lines and open symbols indicate precipitation of NaCl. Data from Pérez-Salado Kamps et al.[62] [Color figure can be viewed in the online issue, which is available at wileyonlinelibrary.com.]

The origin of this discrepancy may be that the presented model does not include the effect of ion-solvent association and in particular the effect on the solvent structure. Additional physics could improve the predictions. It is, however, evident from Figure 21 that including ion hydration through the Wertheim theory, using the procedure presented by Maribo-Mogensen et al.,[23] is not adequate. This is because the calculated effect is not sufficiently large to ensure reduction of the apparent molar volume by over 60% when reasonable hydration numbers are used for the Na^+ and Cl^- ions, indicating that the apparent molar compression from ion solvation should be larger than what is obtained by the present model.

To be able to obtain reasonable agreement with apparent molar volumes, while retaining the covolume parameters calculated from ionic radii, it is suggested to introduce a Peneloux volume translation as shown in Eq. 30 to improve the results

$$v = v^{\mathrm{EoS}} + \sum_i x_i c_i \tag{30}$$

The Peneloux volume correction term can be adjusted to match the experimental data for the apparent molar volume at the solubility limit, leading to excellent representation of the densities of aqueous solutions as shown in Figure 22.

On the role of the static permittivity

In previous work,[11,22,23] the authors showed that static permittivity is the most important property for the electrostatics terms of primitive electrolyte models. Figure 23 shows the predicted static permittivity with e-CPA at 25°C using the same parameters used to produce Figure 2. It is evident that the predicted static permittivity is in good agreement with the experimental data, provided that the effect of kinetic depolarization is taken into account using the model by Hubbard et al.[72] assuming no-slip conditions in Eq. 31[23]

$$\Delta\varepsilon_D = -\left(1-\frac{\varepsilon_\infty}{\varepsilon_r}\right)\frac{\tau\sigma_{DC}}{\varepsilon_0} \tag{31}$$

In which τ is the relaxation time of water, and σ_{DC} is the direct current conductivity of aqueous NaCl solutions. Notice that this result was achieved without taking into account ion solvation, indicating that the trends of the static permittivity can still be well predicted, despite the poor correspondence with liquid densities due to the neglect of ion-solvent association.

Prediction of temperature dependence from infinite dilution heat capacity

While the excess properties at infinite dilution can be modeled using the Debye–Hückel limiting law (see e.g., the activity coefficients in Figure 2), the aqueous standard state properties (at infinite dilution in water) can be modeled using an EoS following Eqs. 32 and 32

$$\Delta_f G^{aq} = \Delta_f G^{ig} + RT_{\mathrm{ref}} \ln\varphi_i^{\infty}(T_{\mathrm{ref}}, P_{\mathrm{ref}}) \tag{32}$$

$$\Delta_f H^{aq} = \Delta_f H^{ig} - RT_{\mathrm{ref}}^2\left(\frac{\partial \ln\varphi_i^{\infty}(T_{\mathrm{ref}}, P_{\mathrm{ref}})}{\partial T}\right) \tag{33}$$

The standard state properties in activity models for electrolytes can be calculated using the Helgeson–Kirkham–Flowers (HKF) model.[73] It consists of a Born-type term for electrostatic interactions (following Eq. 12) but additionally

Table 7. Setschenow Coefficients for Nonelectrolytes and Interaction Parameters with Salt and Water

	k_s @ 25°C (kg/mol)	Interaction with NaCl $\Delta U_{si}/R$ (K)	Interaction with Water (T in K)
Methane	0.152	1128	$k_{ij} = 0.7988 - 236.5/T$
Carbon dioxide	0.110	724.8	$k_{ij} = -0.0232$
Pentane	0.221	811.2	$k_{wi} = 0.0615$
Benzene	0.195	664.2	$k_{wi} = 0.0355$ $\beta_{cross} = 0.079$
Toluene	0.225	643.7	$k_{wi} = 0.0095$ $\beta_{cross} = 0.06$

CH_4 and CO_2 Setschenow coefficients were calculated from the ion-based model from Schumpe,[56] while the Setschenow coefficients for the heavier hydrocarbons were obtained from Xie et al.[57]

treats nonelectrostatic interactions by including additional empirical terms, that take into account the temperature and pressure dependence of the heat capacity and apparent molar volumes. At 1 bar, the contribution to the heat capacity is given by Eq. 34

$$\Delta_{\text{non-Born}}\bar{C}_p^o = c_1 + \frac{c_2}{(T-\Theta)^2} \tag{34}$$

where $c_{1\text{-}2}$ are additional ion-specific parameters and $\Theta = 228$K. Akinfiev et al.[74] fitted parameters for NaCl at 1 bar from experimental heat capacity data down to −30°C, and found that $c_1 = 63.9681$ and $c_2 = -431.167$. Traditionally, the HKF-model is used to determine standard state properties, while an activity coefficient model for the liquid phase is used to describe electrolyte solutions. While empirical models using the HKF approach can be used to correct the apparent molar heat capacity in water, Figure 24 shows that a more fundamental approach is needed to describe the behavior of the heat capacity in other solvents, where the temperature/pressure trends may differ significantly from that of water.

While the model presented in this article satisfactorily captures the effect of the electrical field due to the detailed physical model for the static permittivity, it fails to reproduce the maximum in the apparent molal heat capacity, indicating that the ion-solvent interactions and especially the structural effects should be improved. To predict the temperature-dependent properties, it is proposed to use the standard state heat capacity corrected for the structural effects (represented by the HKF-model) as these cannot be captured by the e-CPA model. When using the $\alpha = 1573$ obtained from a fit to osmotic and activity coefficients for NaCl, the apparent molal heat capacity at 25°C is calculated as −338 J/mol/K (using the mono-atomic ideal gas heat

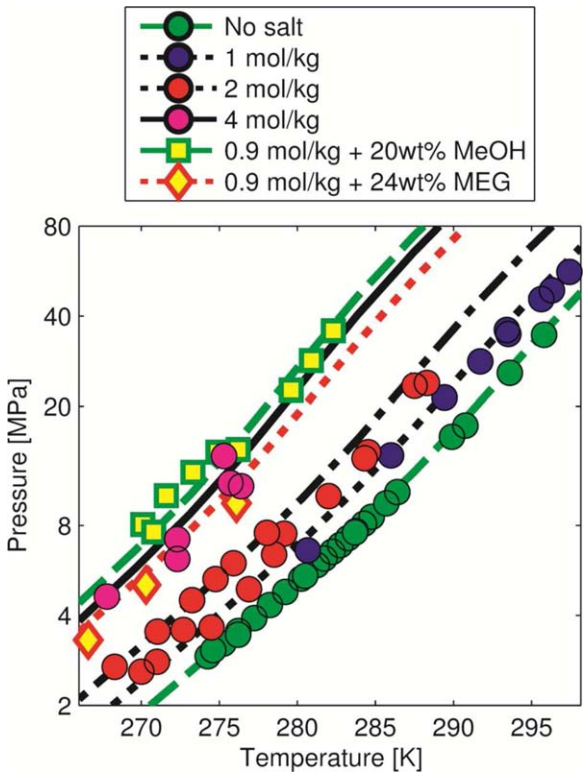

Figure 19. Predicted effect of NaCl on the gas hydrate formation pressure in pure water and mixtures with methanol and ethylene glycol.

Data was obtained from the NIST (2014) Clathrate Hydrate Database.[68] Note that the pressure scale is logarithmic. [Color figure can be viewed in the online issue, which is available at wileyonlinelibrary.com.]

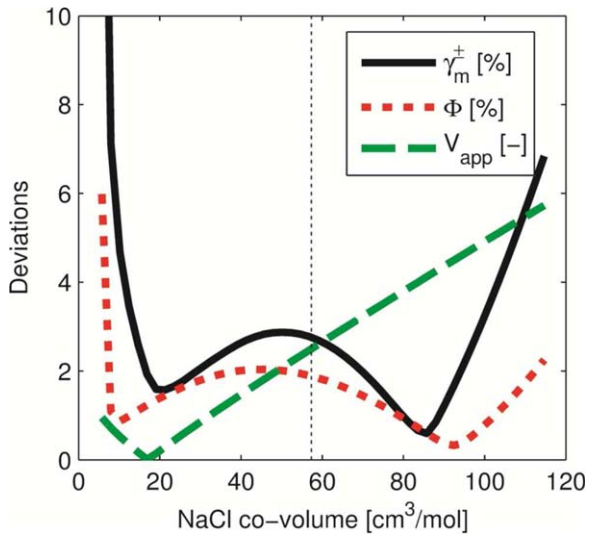

Figure 20. Relative average deviations of mean ionic activity coefficients, osmotic coefficients, and apparent molar volumes at 25°C after fitting the salt-water interaction parameter ΔU_{sw}.

The covolume predicted from Pauling ion diameters of Na^+ and Cl^- is indicated by the vertical dashed line. Note that the deviations in apparent molar volume are given in fraction rather than percentage to fit in the y axis scale. [Color figure can be viewed in the online issue, which is available at wileyonlinelibrary.com.]

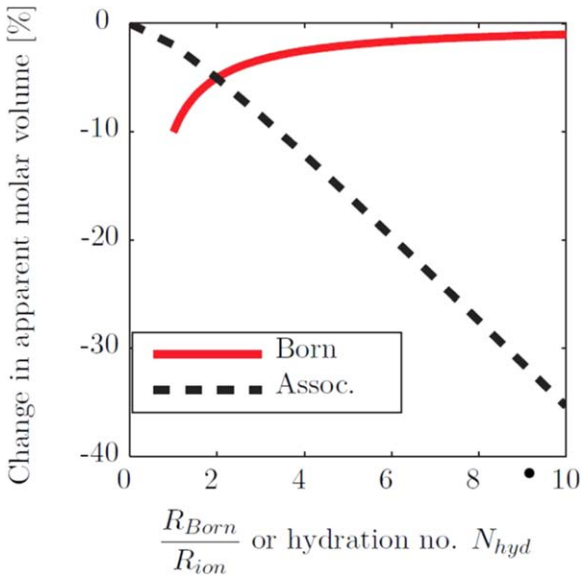

Figure 21. Effect of hydration number and Born radius on the apparent molar volume of NaCl at infinite dilution.

[Color figure can be viewed in the online issue, which is available at wileyonlinelibrary.com.]

capacity of 20.78 J/mol/K for Na^+ and Cl^-), which is clearly too low even when the structural effects to the heat capacity at 25°C are subtracted. If we instead adjust $\alpha_i = 705$K the model matches the corrected heat capacity $C^{\infty}_{p,e}$ (25°C) = −147.88 J/mol/K, it becomes possible to get a good correspondence with standard state heat capacities, enthalpies and volumes as presented in Figure 25. It is evident that the heat capacity up to high temperatures is predicted well by this model and that the model also predicts the pressure dependence, except at the low temperatures, where also the HKF-model had to be extended.

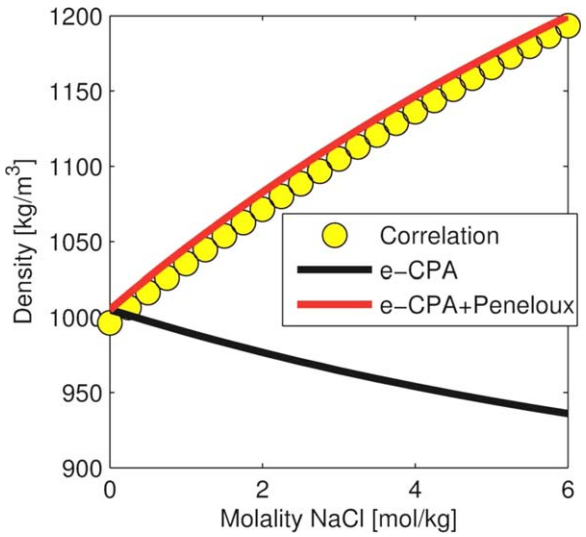

Figure 22. Liquid densities calculated from the correlation by Al Ghafri et al.[69] in comparison to results from e-CPA with and without a Peneloux volume translation.

[Color figure can be viewed in the online issue, which is available at wileyonlinelibrary.com.]

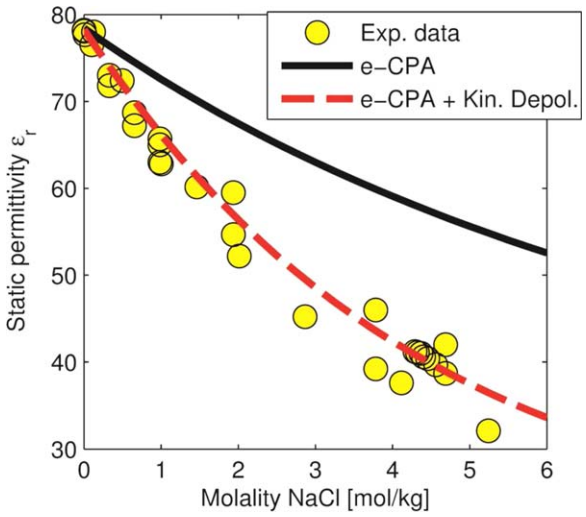

Figure 23. Dielectric constant of NaCl at 25°C based on e-CPA predictions with and without including the effect of kinetic depolarization from Eq. 31 using.

The kinetic depolarization effect is calculated from Eq. 30 using experimental conductivities from the CRC Handbook of Chemistry and Physics[70] and 8.7ps as the dielectric relaxation time for pure water at 20°C (Rønne et al.[71]). [Color figure can be viewed in the online issue, which is available at wileyonlinelibrary.com.]

The authors note that a complete electrolyte EoS should be able to capture both infinite dilution and excess properties in any medium (water, methanol, or in a mixed solvent), but that it would require further model development to account for the structural effects leading to the maximum in the apparent molar heat capacity/volume. While this approach has not been pursued in this article, the authors note that the characteristic maximum in the apparent molar heat capacity

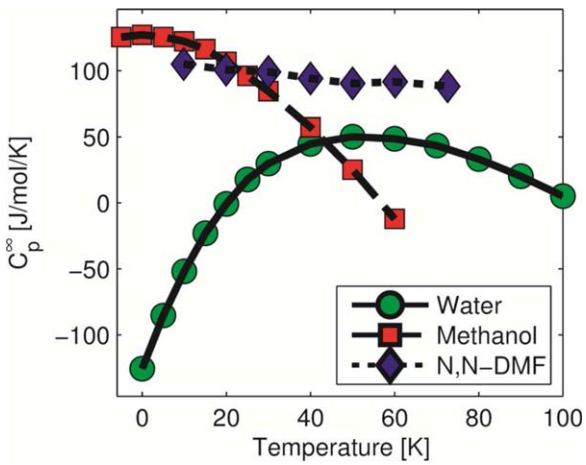

Figure 24. Apparent molar heat capacities of NaClO4 at infinite dilution in water, methanol, and *N,N*-dimethylformamide from Mastroianni and Criss[75] and Chang and Criss.[76]

The lines are guides for the eye and not modeling results. [Color figure can be viewed in the online issue, which is available at wileyonlinelibrary.com.]

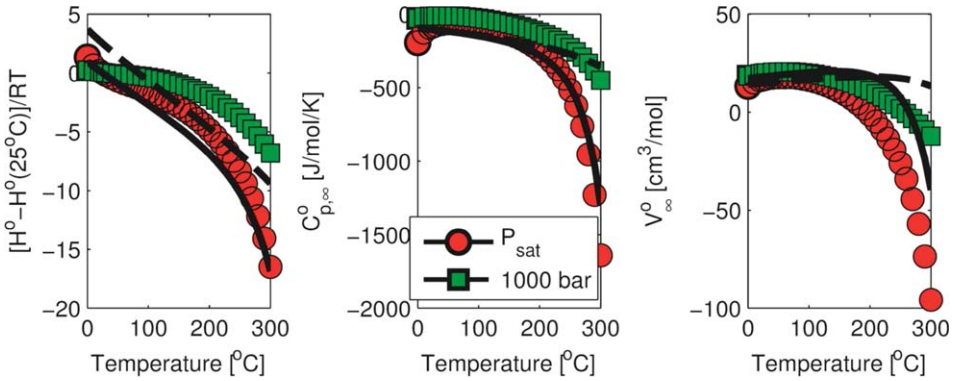

Figure 25. Standard state properties of NaCl at infinite dilution in water when α is fitted to the heat capacity at 25°C corrected for structural effects that cannot be captured by the model.

Note that the apparent molar volume at infinite dilution includes the Peneloux volume correction. Circles and squares are from the model by Pitzer et al.[48] and the lines are from e-CPA. Red circles and solid black line correspond to the predictions from the two models at the saturation pressure of water. Green squares and dashed lines correspond to the predictions from the two models at 1000 bar. In all cases symbols indicate calculations with the Pitzer model and lines with e-CPA. [Color figure can be viewed in the online issue, which is available at wileyonlinelibrary.com.]

qualitatively resembles the results with the MB model for argon at infinite dilution in water.[77]

Salt effect on liquid-liquid equilibrium

For many miscible azeotropic mixtures (such as water + 1-propanol), the presence of salts can introduce a liquid-liquid split. This behavior may also be calculated using the e-CPA EoS where the salt-propanol interaction coefficient shown in Table 6 has been estimated based on the solubility of 1-propanol in water as a function of the salt concentration. Figure 26 shows that while the model captures reasonably well the overall solubility of NaCl, the solubility of NaCl in the iso-propanol rich phase is greatly underestimated. This problem may be attributed to the lack of accounting for ion-ion association, in which case the Na^+ and Cl^- ions would recombine and form a neutral ion pair. Liquids with lower static permittivity will have a higher propensity of ion pair formation, and this will thus increase the driving force for Na+ and Cl− toward the organic phase.

General discussion

In this work, we have presented a novel approach for correlating and predicting thermodynamic properties of electrolyte mixtures with water and in mixed solvents. A simple scheme for parameterization of the EoS to obtain salt-solute or salt-solvent interaction parameters was presented, and these parameters were subsequently used to predict diverse types of phase equilibrium, including VLE, LLE, SLE (including gas hydrates) in mixed solvents, as well as the densities of mixtures of water, methanol, NaCl, and Na_2SO_4. The relationship between ion-specific and salt-specific parameters shown in Eq. 16 can be used in general to simplify the application to various systems, including gases, mixed solvents, and mixed salts. However, when the number of possible salts exceeds the number of ions, the parameters must be re-estimated to obtain the best fit to all salt data. This may require the introduction of additional ion-ion interaction parameters, and will also require estimation of ion-specific interaction parameters between other solutes and

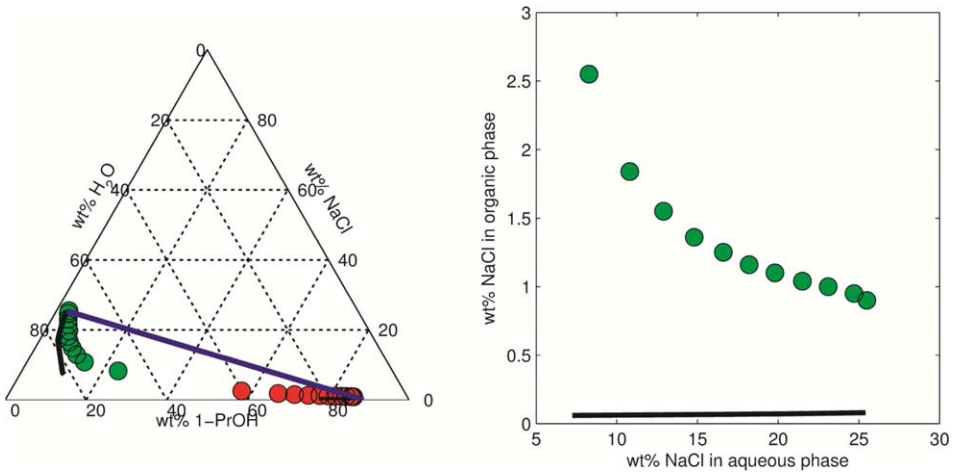

Figure 26. Liquid-liquid equilibrium of water + 1-propanol at 25°C in the presence of NaCl using the parameters from Table 6.

Experimental data from De Santis et al.[78] [Color figure can be viewed in the online issue, which is available at wileyonlinelibrary.com.]

solvents. Such parameterizations have been performed for other equations of state, but they have not been applied to all types of relevant phase equilibrium, and the parameterization has typically only involved a limited number of salts. The purpose of this work was to demonstrate the feasibility of the e-CPA approach, in which the static permittivity is determined from the model presented in Maribo-Mogensen et al.,[23] and this has been largely successful.

The simplified model has demonstrated that by neglecting the ion-solvent association the model can still obtain good agreement with thermodynamic properties, but not the volumetric data. By introducing a Peneloux volume translation, it is possible to achieve good correspondence with densities in water, whereas the densities in mixed solvents are modeled to a lower degree of accuracy as evidenced by Figure 13.

The relatively poor agreement with the solubility of NaCl in the propanol-rich phase for the liquid-liquid equilibrium with water (Figure 26) indicates that ion-ion association would become important to get proper agreement with both phases. Since ion-ion association would be more prevalent in the phase with lowest static permittivity, this would in turn increase the solubility of NaCl in propanol.[79]

Conclusions

This work has demonstrated the feasibility of the e-CPA EoS for thermodynamic modeling of mixed solvent systems containing salts. The model extends the functionality of the Cubic Plus Association EoS to salts (while maintaining compatibility with existing parameters) by including the Debye–Hückel and Born terms combined with a new model for a self-consistent calculation of the static permittivity of the fluid. As the model furthermore reduces to the Soave–Redlich–Kwong equation, it is also compatible with existing tools for characterized petroleum fractions, and is therefore suited for handling phase equilibrium calculations in the presence of oil, gas, brine, and chemicals. The model can be parameterized based on either ion- or salt-specific parameters, and this flexibility can greatly simplify the thermodynamic modeling of mixtures with limited number of ions. A simple temperature dependence of the ion-solvent interaction parameter enables prediction of thermodynamic properties of complex mixtures over wide temperature and pressure ranges.

Acknowledgment

The authors wish to thank Statoil and Gassco (Norway), BP International Limited (UK) and Petrobras (Brazil) for supporting this work as part of the CHIGP project (Chemicals in Gas Processing).

Literature Cited

1. Hendriks E, Kontogeorgis G, Dohrn R, de Hemptinne J-C, Economou I, Zilnik L, Vesovic V. Industrial requirements for thermodynamics and transport properties. *Ind Eng Chem Res*. 2010;49:11131–11141.
2. Kontogeorgis G, Folas G. *Thermodynamic Models for Industrial Applications: From Classical and Advanced Mixing Rules to Association Theories*. Chippenham, UK: Wiley, 2010.
3. Chen C, Mathias P. Applied thermodynamics for process modeling. *AIChE J*. 2002;48:194–200.
4. Chen C-C, Song Y. Extension of nonrandom two-liquid segment activity coefficient model for electrolytes. *Ind Eng Chem Res*. 2005;44:8909–8921.
5. Wang P, Springer RD, Anderko A, Young RD. Modeling phase equilibria and speciation in mixed-solvent electrolyte systems. *Fluid Phase Equilib*. 2004;222–223:11–17.
6. Pitzer KS. Electrolyte theory—improvements since Debye and Hückel. *Acc Chem Res*. 1977;10:371–377.
7. Prausnitz JM, Lichtenthaler RN, de Azevedo EG. *Molecular Thermodynamics of Fluid-Phase Equilibria*, 3rd ed. Upper Saddle River, NJ: Prentice Hall Int., 1999.
8. Debye P, Hückel E. Zur Theorie der Elektrolyte. *Phys Z*. 1923;24:179–207.
9. Blum L. Mean spherical model for asymmetric electrolytes: I. *Method of solution. Mol Phys*. 1975;30:1529–1535.
10. Herzog S, Gross J, Arlt W. Equation of state for aqueous electrolyte systems based on the semirestricted non-primitive mean spherical approximation. *Fluid Phase Equilib*. 2010;297:23–33.
11. Maribo-Mogensen B, Kontogeorgis G, Thomsen K. Comparison of the Debye-Huckel and the mean spherical approximation theories for electrolyte solutions. *Ind Eng Chem Res*. 2012;51:5353–5363.
12. Van't Hoff J. 1901. Osmotic pressure and chemical equilibrium. Nobel Lecture 13.
13. McMillan W Jr, Mayer J. The statistical mechanics of multicomponent solutions. *J Chem Phys*. 1945;13:276–305.
14. Adelman S. The effective direct correlation function, an approach to the theory of liquid solutions: a new definition of the effective solute potential. *Chem Phys Lett*. 1976;38:567–570.
15. Adelman S. The effective direct correlation function: an approach to the theory of liquid solutions. *J Chem Phys*. 1976;64:724–731.
16. Wertheim M. Exact solution of the mean spherical model for fluids of hard spheres with permanent electric dipole moments. *J Chem Phys*. 1971;55:4291–4298.
17. Liu Z, Li Y, Lu J. Low-density expansion of the solution of mean spherical approximation for ion-dipole mixtures. *J Phys Chem B*. 2002;106:5266–5274.
18. Liu Z, Wang W, Li Y. An equation of state for electrolyte solutions by a combination of low-density expansion of non-primitive mean spherical approximation and statistical associating fluid theory. *Fluid Phase Equilib*. 2005;227:147–156.
19. Born M. Volumen und hydratationswärme der ionen. *Z Phys A Hadrons Nuclei*. 1920;1:45–48.
20. Myers J, Sandler S, Wood R. An equation of state for electrolyte solutions covering wide ranges of temperature, pressure, and composition. *Ind Eng Chem Res*. 2002;41:3282–3297.
21. Inchekel R, de Hemptinne J-C, Fürst W. The simultaneous representation of dielectric constant, volume and activity coefficients using an electrolyte equation of state. *Fluid Phase Equilib*. 2008;271:19–27.
22. Maribo-Mogensen B, Kontogeorgis G, Thomsen K. Modeling of dielectric properties of aqueous salt solutions with an equation of state. *J Phys Chem B*. 2013;117:10523–10533.
23. Maribo-Mogensen B, Kontogeorgis G, Thomsen K. Modeling of dielectric properties of complex fluids with an equation of state. *J Phys Chem B*. 2013;117:3389–3397.
24. Onsager L. Electric moments of molecules in liquids. *J Am Chem Soc*. 1936;58:1486–1493.
25. Kirkwood J. Theoretical studies upon dipolar ions. *Chem Rev*. 1939;24:233–251.
26. Frölich H. *Theory of Dielectrics*. Oxford: Clarendon Press, 1949.
27. Kontogeorgis G, Voutsas E, Yakoumis I, Tassios D. An equation of state for associating fluids. *Ind Eng Chem Res*. 1996;35:4310–4318.
28. Marcus Y. Electrostriction in electrolyte solutions. *Chem Rev*. 2011;111:2761–2783.
29. Chapman W, Gubbins K, Jackson G, Radosz M. SAFT: equation-of-state solution model for associating fluids. *Fluid Phase Equilib*. 1989;52:31–38.
30. Michelsen M. Robust and efficient solution procedures for association models. *Ind Eng Chem Res*. 2006;45:8449–8453.
31. Michelsen M, Hendriks E. Physical properties from association models. *Fluid Phase Equilib*. 2001;180:165–174.
32. Wu J, Prausnitz JM. Phase equilibria for systems containing hydrocarbons, water, and salt: an extended Peng-Robinson equation of state. *Ind Eng Chem Res*. 1998;37:1634–1643.
33. Lee BS, Kim KC. Modeling of aqueous electrolyte solutions based on perturbed-chain statistical associating fluid theory incorporated with primitive mean spherical approximation. *Korean J Chem Eng*. 2009;26:1733–1747.

34. Raatschen W, Harvey AH, Prausnitz JM. Equation of state for solutions of electrolytes in mixed solvents. *Fluid Phase Equilib*. 1987; 38:19–38.
35. Harvey AH, Prausnitz JM. Thermodynamics of high-pressure aqueous systems containing gases and salts. *AIChE J*. 1989;35:635–644.
36. Lin Y, Thomsen K, de Hemptinne JC. Multicomponent equations of state for electrolytes. *AIChE J*. 2007;53:989–1005.
37. Haghtalab A, Mazloumi SH. A square-well equation of state for aqueous strong electrolyte solutions. *Fluid Phase Equilib*. 2009;285: 96–104.
38. Haghtalab A, Mazloumi SH. Electrolyte cubic square-well equation of state for computation of the solubility CO2 and H2S in aqueous MDEA solutions. *Ind Eng Chem Res*. 2010;49:6221–6230.
39. Rozmus J, de Hemptinne JC, Galindo A, Simon D, Mougin P. Modelling of strong electrolytes with ePPC-SAFT up to high temperatures. *Ind Eng Chem Res*. 2013;52:9979–9994.
40. Zuber A, Checoni RF, Mathew R, Santos JPL, Tavares FW, Castier M. Thermodynamic properties of 1: 1 salt aqueous solutions with the electrolattice equation of state. *Oil Gas Sci Technol Revue d'IFP Energies nouvelles*. 2013;68:255–270.
41. Zuber A, Checoni RF, Castier M. Thermodynamic properties of aqueous solutions of single and multiple salts using the Q-electrolattice equation of state. *Fluid Phase Equilib*. 2014;362:268–280.
42. Marcus Y. Thermodynamics of solvation of ions. Part 5. Gibbs free energy of hydration at 298.15 K. *J Chem Soc Faraday Trans*. 1991; 87:2995–2999.
43. Mejıas JA, Lago S. Calculation of the absolute hydration enthalpy and free energy of H+ and OH−. *J Chem Phys* 2000;113:7306–7316.
44. Wagman DD, Evans WH, Parker VB, Schumm RH, Halow I, Bailey SM, Churney KL, Nuttall RL. The NBS tables of chemical thermodynamic properties. Selected values for inorganic and C, and C, organic substances in SI units. *J Phys Chem Ref Data, Suppl*. 1982; 11:2.<≫
45. Thomsen K, Rasmussen P, Gani R. Correlation and prediction of thermal properties and phase behaviour for a class of aqueous electrolyte systems. *Chem Eng Sci*. 1996;51:3675–3683.
46. Cobble JW, Murray RC, Sen U. Field and structure behaviour of electrolytes. *Nature*. 1981;291:566–568.
47. Thomsen K. CERE Electrolyte Database. 2014. Available at http://www.cere.dtu.dk/Expertise/Data_Bank/Search. Accessed on February, 2015.
48. Pitzer K, Peiper JC, Busey RH. Thermodynamic properties of aqueous sodium chloride solutions. *J Phys Chem Ref Data*. 1984;13:1–102.
49. Saad D, Padova J, Marcus Y. Thermodynamics of mixed electrolyte solutions. VI. An isopiestic study of a pseudo-ternary system: NaCl-KCl-MgCl2-H2O at 25°C. *J Solut Chem*. 1975;4:983–993.
50. Rard JA, Clegg SL, Platford RF. Thermodynamics of {z NaCl + (1-z) Na2SO4}(aq) from T = 278.15K to T = 318.15 K, and representation with an extended ion-interaction (Pitzer) model. *J Chem Thermodyn*. 2003;35:967–1008.
51. von Solms N, Michelsen M, Passos C, Derawi S, Kontogeorgis G. Investigating models for associating fluids using spectroscopy. *Ind Eng Chem Res*. 2006;45:5368–5374.
52. Pinho SP, Macedo EA. Representation of salt solubility in mixed solvents: a comparison of thermodynamic models. *Fluid Phase Equilib*. 1996;116:209–216.
53. Emons HH, Röser H. Untersuchungen an Systemen aus Salzen und gemischten Lösungsmitteln. III. Die Beeinflussung der Systeme Kaliumsulfat-bzw. Natriumsulfat-Alkohol-Wasser durch Zusatz von Natrium-oder Kaliumchlorid. *Z anorganische allg Chem*. 1967;353: 135–147.
54. Pinho SP, Macedo EA. Solubility of NaCl, NaBr, and KCl in water, methanol, ethanol, and their mixed solvents. *J Chem Eng Data*. 2005;50:29–32.
55. Djamali E, Kan AT, Tomson MB. A priori prediction of thermodynamic properties of electrolytes in mixed aqueous–organic solvents to extreme temperatures. *J Phys Chem B*. 2012;116:9033–9042.
56. Schumpe A. The estimation of gas solubilities in salt solutions. *Chem Eng Sci*. 1993;48:153–158.
57. Xie WH, Shiu WY, Mackay D. A review of the effect of salts on the solubility of organic compounds in seawater. *Mar Environ Res*. 1997;44:429–444.
58. Price L. Aqueous solubility of petroleum as applied to its origin and primary migration. *AAPG Bull*. 1976;60:213–244.
59. O'Sullivan T, Smith N. Solubility and partial molar volume of nitrogen and methane in water and in aqueous sodium chloride from 50 to 125. deg. and 100 to 600 atm. *J Phys Chem*. 1970;74:1460–1466.
60. Rumpf B, Nicolaisen H, Öcal C, Maurer, G. Solubility of carbon dioxide in aqueous solutions of sodium chloride: experimental results and correlation. *J Solut Chem*. 1994;23:431–448.
61. Kiepe J, Horstmann S, Fischer K, Gmehling J. Experimental determination and prediction of gas solubility data for CO2+ H2O mixtures containing NaCl or KCl at temperatures between 313 and 393 K and pressures up to 10 MPa. *Ind Eng Chem Res*. 2002;41: 4393–4398.
62. Pérez-Salado Kamps A, Jödecke M, Xia J, Vogt M, Maurer G. Influence of salts on the solubility of carbon dioxide in (water+ methanol). Part 1: sodium chloride. *Ind Eng Chem Res*. 2006;45:1505–1515.
63. Karakatsani E, Kontogeorgis G. Thermodynamic modeling of natural gas systems containing water. *Ind Eng Chem Res*. 2013;52:3499–3513.
64. Van der Waals J, Platteeuw J. Clathrate solutions. *Adv Chem Phys*. 1959;2:1–57.
65. Sloan E, Koh C. *Clathrate hydrates of natural gases*. Boca Raton, FL: CRC Press, 2007.
66. Avlonitis D. The determination of Kihara potential parameters from gas hydrate data. *Chem Eng Sci*. 1994;49:1161–1173.
67. Parrish W, Prausnitz J. Dissociation pressures of gas hydrates formed by gas mixtures. *Ind Eng Chem Process Des Dev*. 1972;11:26–35.
68. NIST. NIST Clathrate Hydrate Physical Property Database, Boulder, Colorado: Thermodynamics Research Center (TRC), 2014.
69. Al Ghafri S, Maitland GC, Trusler JPM. Densities of aqueous MgCl2(aq), CaCl2(aq), KI(aq), NaCl(aq), KCl(aq), AlCl3(aq), and (0.964 NaCl+00136 KCl)(aq) at temperatures between (283 and 472) K, pressures up to 68.5 MPa, and molalities up to 6 mol.kg(-1). *J Chem Eng Data*. 2012;57:1288–1304.
70. Haynes W. *CRC Handbook of Chemistry and Physics*, 93rd ed. Boca Raton, FL: CRC Press, 2014.
71. Rønne C, Thrane L, Åstrand PO, Wallqvist A, Mikkelsen KV, Keiding SR. Investigation of the temperature dependence of dielectric relaxation in liquid water by THz reflection spectroscopy and molecular dynamics simulation. *J Chem Phys*. 1997;107:5319–5331.
72. Hubbard JB, Onsager L, Van Beek WM, Mandel M. Kinetic polarization deficiency in electrolyte solutions. *Proc Natl Acad Sci U S A*. 1977;74:401–404.
73. Johnson JW, Oelkers EH, Helgeson HC. SUPCRT92: a software package for calculating the standard molal thermodynamic properties of minerals, gases, aqueous species, and reactions from 1 to 5000 bar and 0 to 1000 *C*. *Comput Geosci*. 1992;18:899–947.
74. Akinfiev NN, Mironenko MV, Grant SA. *Thermodynamic properties of NaCl solutions at subzero temperatures. J Solut Chem*. 2001;30: 12.
75. Mastroianni MJ, Criss CM. Standard partial molal heat capacities of sodium perchlorate in water from 0-90°C and in anhydrous methanol from -5-55°*C*. *J Chem Eng Data*. 1972;17:222–226.
76. Chang S, Criss CM. Partial molal heat capacities of sodium perchlorate in N,N-dimethylformamide from 10 to 75°*C*. *J Solut Chem*. 1973;2:457–466.
77. Ben-Naim A. *Solvation Thermodynamics*. Oxford, UK: Kluwer Academic, 1987.
78. De Santis R, Marrelli L, Muscetta P. Liquid-liquid equilibria in water-aliphatic alcohol systems in the presence of sodium chloride. *Chem Eng J*. 1976;11:207–214.
79. Holovko M. Concept of ion association in the theory of electrolyte solutions. In: *Ionic Soft Matter: Modern Trends in Theory and Applications*. AA Dordrecht, The Netherlands: Springer, 2005:45–81.

Manuscript received Nov. 28, 2014, and revision received Mar. 17, 2015.